RECLAMATION

Managing Water in the West

Technical Report No. SRH-2013-09

Coupled 2D Morpho-Dynamic and Bank Erosion Modeling at the Upper Junction City Channel Rehabilitation Project Site, Trinity River, CA

U.S. Department of the Interior
Bureau of Reclamation
Technical Service Center
Denver, Colorado

March 2013

Mission Statements

The mission of the U.S. Department of the Interior is to protect America's natural resources and heritage, honors our cultures and tribal communities, and supplies the energy to power our future.

The mission of the Bureau of Reclamation is to manage, develop, and protect water and related resources in an environmentally and economically sound manner in the interest of the American public.

Cover Photo: Taken in August 2012 when the project was under construction

Technical Report No. SRH-2013-09

Coupled 2D Morpho-Dynamic and Bank Erosion Modeling at the Upper Junction City Channel Rehabilitation Project Site, Trinity River, CA

Report Prepared by:

Yong G. Lai, Ph.D., Hydraulic Engineer
Sedimentation and River Hydraulics Group, Technical Service Center

U.S. Department of the Interior
Bureau of Reclamation
Technical Service Center
Denver, Colorado

Peer Review Certification: This document has been peer reviewed per guidelines established by the Technical Service Center and is believed to be in accordance with the service agreement and standards of the profession. Questions concerning this report should be addressed to Timothy Randle, Group Manager of the Sedimentation and River Hydraulics Group (86-68240) at 303-445-2557.

PREPARED BY:

_____ DATE:_____

Yong Lai, Ph.D.
Hydraulic Engineer
Sedimentation and River Hydraulics Group (86-68240)

PEER REVIEWED BY:

_____ DATE:_____

Blair P. Greimann, Ph.D.
Hydraulic Engineer
Sedimentation and River Hydraulics Group (86-68240)

Table of Contents

Index of Figures

Page

Index of Tables

Page

Executive Summary

Sedimentation and River Hydraulics Group (SRHG) at the Technical Service Center of Reclamation was tasked with providing technical assistance for a coupled morpho-dynamic and bank erosion modeling of the Trinity River reach at the Upper Junction City (UJC). The primary objective of the study was to test and verify an advanced modeling tool to the prediction of potential channel morphological changes at the UJC site so that such a tool might be of use for Trinity River restoration and rehabilitation projects in the future. The work was part of a joint effort among Reclamation's Trinity River Restoration Program (TRRP), Cardno ENTRIX, and SRHG. Engineers at TRRP initiated SRH-2D modeling at the UJC site who provided much needed initial data for the current SRHG study. A separate field study and modeling with BSTEM, Bank-Stability and Toe-Erosion Model (Simon et al. 2000; 2011), were carried out by Cardno ENTRIX. The Cardno ENTRIX (2012) study provided bank properties and modeling results.

Three tasks were carried out with the SRHG study contained in this report. They are described with major study findings summarized.

Task 1 was to modify the existing SRH-2D model to accept the BSTEM-predicted bank-generated sediment loadings as lateral inputs for stream transport. A series of model runs were carried out to get quick turn-around results to assess the impact of the design construction on stream morphology. BSTEM-predicted sediment loadings at ten bank cross sections were used as model inputs. The objective of Task 1 was to see whether the existing SRH-2D, without the coupled morpho-dynamic and bank erosion modeling, might be sufficient for project applications.

Major Conclusions of Task 1 Study: Comparisons of the Task 1 results with those based on the coupled morpho-dynamic and bank erosion modeling showed that some of the conclusions of the coupled modeling were reproduced with the SRH-2D modeling with the BSTEM-generated bank sediment loadings. However, there were others which were different. The differences between the two were large enough that the coupled model was recommended when measured data of bank properties was available.

Task 2 was to carry out a coupled morpho-dynamic and bank erosion modeling for the purpose of model calibration and verification. The primary objective was to find out whether the advanced coupled modeling might be of use for Trinity River restoration and rehabilitation projects in the future. For the latest development of the coupled morpho-dynamic and bank erosion modeling in SRH-2D, readers may refer to the papers by Lai et al. (2012a; 2012b). The initial plan

of the task was to use the BSTEM model as the bank erosion model in the coupled modeling. However, it was found during the study that the most significant bank retreat section of the UJC site consisted of primarily uniform and non-cohesive banks based on the data in the Cardno ENTRIX (2012) study. It was decided, therefore, that the linear retreat non-cohesive bank erosion model was adopted instead of the BSTEM model with the coupled modeling.

Major Conclusions of Task 2 Study: The calibration and verification modeling runs were carried out under the 2009 "pre-erosion baseline" condition; model results were compared with the 2011 terrain data. The necessary bank erosion model inputs, mainly the critical shear stress and erodibility, were taken from the field measured and/or BSTEM estimated data. Figure E1 is the terminology used for the bank erosion section and stream pools. The following conclusions may be drawn based on the Task 2 model results:

- The coupled model was capable of predicting the retreat of the bank erosion zone (see Figure E1) using the field measured and BSTEM calibrated bank parameters.
- Addition of the bank erosion sediments to the stream did not impact channel morphology upstream of the bank erosion zone appreciably. The eroded bank sediments deposited in the stream stayed near the banks and were not transported to downstream very far, at least during the simulation period (2009 through 2011). The predicted deposition in the nearby stream was confirmed based on the measured 2009 and 2011 terrain data.
- The coupled model was capable of predicting the qualitative erosion and deposition patterns in the study reach.
- There were, however, two main discrepancies between the model predictions and the measured data. First, the model predicted much more deposition than the measurement in the three pools in Figure E1. Second, the riffle vertical erosion downstream of Pool 2 was not predicted by the model. The over-prediction of the pool filling process has been a consistent problem with any depth-averaged numerical models since such models did not take the horizontal vortices into consideration. The riffle erosion downstream of Pool 2 was predicted when runoff peak was below 7,500 cfs but missed by the model when the flow was above12,000 cfs. The most probable cause was conjectured to be the existing mature vegetation along the nearby right bank which was under water only at high discharges in 2011 but not represented by the model.

It is concluded that the coupled model used in the present study may be used to assess the impact of the rehabilitation project on morphologic processes such as bank erosion and bed changes of both the main and side channels. The model is in adequate in predicting the pool-filling process.

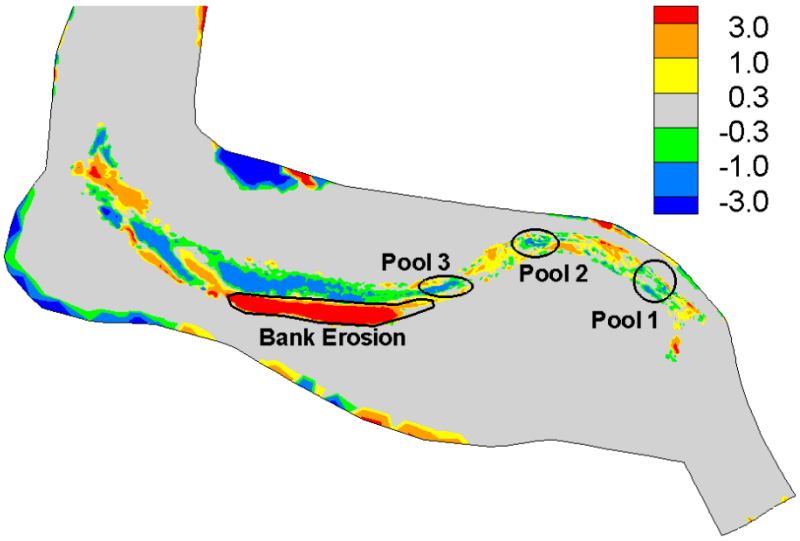

Figure E1. Figure for the terminology used to identify the bank erosion section and pools with the design construction.

Task 3 was to carry out project impact assessment modeling using the coupled model developed in Task 2. The model runs in this task were named "morphologic assessment" runs. Due to potential uncertainties of numerical models, relative comparison was made between two scenarios to arrive at some conclusions. Relative comparisons are often more accurate than the absolute prediction about channel morphology changes. Two scenarios were simulated under the morphological assessment condition: the 2011 "post-erosion" scenario and the 2012 "design construction" scenario. The design construction condition was modeled, not the actual constructed project since the actual construction data was unavailable at the start of this study (May, 2012). Note that the design construction was only evaluated over a 3-year period and the results reflected only the initial channel responses to the design construction. The ultimate new equilibrium state of the channel was not evaluated. For ease of presentation of the summary results, the terminology used in referring to project locations follows that in Figure E2.

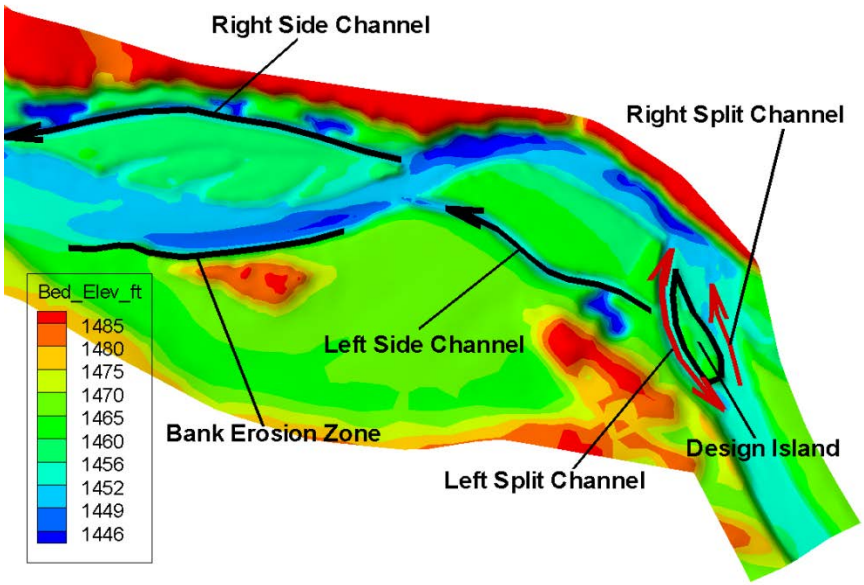

Figure E2. Figure for the terminology used to identify different features of the design construction.

Major Conclusions of Task 3 Study: Major predicted impacts of the design construction on stream morphology are summarized as follows:

- Among the two side channels of the design construction - the upstream left side channel and the downstream right side channel in Figure E2 - the entrance region of the right side channel was predicted to have a risk of deposition. Deposition in this entrance zone, however, would occur only when the flow was above 12,000 cfs.
- A potential impact of the design construction was that the channel downstream of the design island (see Figure E2) might experience less deposition in some areas and more erosion in others, resulting in deeper channels in most areas than the 2011 post-erosion terrain condition. However, the simulated bank erosion zone was not predicted to experience more erosion under the design construction condition; a slight decrease in bank erosion rate was predicted instead.
- The left split channel (see Figure E1) was predicted to experience deposition with the design construction; the deposited sediment size was predicted to be around d_{50} of 15 to 17 mm.

1 Introduction

Sedimentation and River Hydraulics Group (SRHG) at the Technical Service Center of Reclamation was tasked with providing technical assistance for a coupled morpho-dynamic and bank erosion modeling of the Trinity River reach at the Upper Junction City (UJC). The primary objective of the study was to test and verify an advanced modeling tool to the prediction of potential channel morphological changes at the UJC site so that such a tool might be of use for Trinity River restoration and rehabilitation projects in the future. The work was part of a joint effort among Reclamation's Trinity River Restoration Program (TRRP), Cardno ENTRIX, and SRHG. Engineers at TRRP initiated SRH-2D modeling at the UJC site who provided much needed initial data for the current SRHG study. A separate field and BSTEM (Bank-Stability and Toe-Erosion Model) modeling study was carried out by Cardno ENTRIX. The Cardno ENTRIX (2012) study provided bank properties and modeling results that were used as some of the model inputs by the SRHG study. In this report, "channel left" refers to the direction when one looks downstream and "right" is defined the same way.

The project consisted of the following tasks:

Task 1 was to modify the existing mobile-bed SRH-2D model to accept the BSTEM-predicted bank-generated sediment loadings as lateral inputs for stream transport. TRRP provided initial SRH-2D mobile-bed models developed for the UJC site. These initial models did not take bank-generated sediment loadings or bank erosion into consideration. Cardno ENTRIX (2012) study provided BSTEM predicted bank sediment loadings at ten bank cross sections over a time period encompassing the current study. These loadings were in the form of time series data and by size classes. Once SRH-2D was modified to accept the bank-generated sediment loadings, a series of model runs - named "preliminary modeling" (PM) - were carried out in order to get quick turn-around results to assess the project impact.

Task 2 was to carry out a coupled morpho-dynamic and bank erosion modeling. Some of the bank parameters used by the coupled modeling were field measured and/or BSTEM predicted; these data were obtained through an analysis and were documented in Cardno ENTRIX (2012). A fully coupled morpho-dynamic and bank erosion model has been under research and development at Reclamation (SRH-2D) and some results were documented in the papers of Lai et al. (2012a; 2012b). In this task, a calibration study was carried out first at the UJC site using the new SRH-2D model; model results were compared with available 2009 and 2011 bathymetric data. The calibration study ensured the applicability of the coupled model to the study site. All calibration study model runs were named "pre-erosion baseline" (PB) cases. Initially, the intent was to adopt the BSTEM

bank erosion model for the coupled modeling. However, after the bank retreat data from TRRP and bank properties from Cardno ENTRIX (2012) were received, it was decided to use the linear retreat bank erosion model since the significant retreating bank section consisted of mainly uniform and non-cohesive sediments.

Task 3 was to carry out project application studies. Once the coupled model was calibrated and verified in Task 2, the same model was applied to assess the impact of the river rehabilitation project on channel morphology at the UJC site. The "design construction" was modeled, not the actual constructed project. Actual project construction started in June 2012 and was completed in November 2012. The actual construction data was unavailable at the start of this study (May 2012). The model runs in Task 3 were named "morphologic assessment" (MA) cases. Two scenarios were simulated under the MA condition: the 2011 "post-erosion" (PC) scenario and the 2012 "design construction" (DC) scenario.

2 Available Data

2.1 Terrain Data

The bathymetry and topography of the UJC reach were obtained by engineers at TRRP. Two sets of data were obtained from various survey methods before the project implementation: one 2009 data set (the "pre-erosion baseline" condition) and another 2011 data set (the "post-erosion" condition). In addition, the bathymetric and topographic data were also obtained from TRRP representing the "design construction" condition. The three sets of data are displayed in Figure 1 through Figure 3 along with the aerial photos.

The 2009 terrain incorporated data from two sources. Terrestrial and bathymetric LiDAR was flown in early April 2009 before flow started going up for the 2009 release. This data was very good in the emergent areas but poor in the shallow submerged areas. Therefore, sonar data was obtained in areas deeper than about a meter in November to December of 2009. The sonar was in the pools and other deeper areas in the more upstream of the two big bends in the model. The exact dates were not that important because the only time flows were high enough to move gravel or erode banks was during the 2009 release – late April through June or early July. The winter floods did not come until after the sonar was collected.

The 2011 terrain was updated using ground survey data collected on October 4, 2011 along the eroding part of the bank and in the wadable part of the channel where that big bar complex was depositing adjacent to where the bank had eroded a lot (lower half of the site). Additional sonar was conducted on July 7, 1011 in the deeper areas in the upstream bend and through the cross over. The shallow area where the wide bar was near the bridge was covered with a ground survey on Sept. 26 and 27, 2011. Again, nothing much happened between the spring release and the winter storms that usually did not come until late December or January.

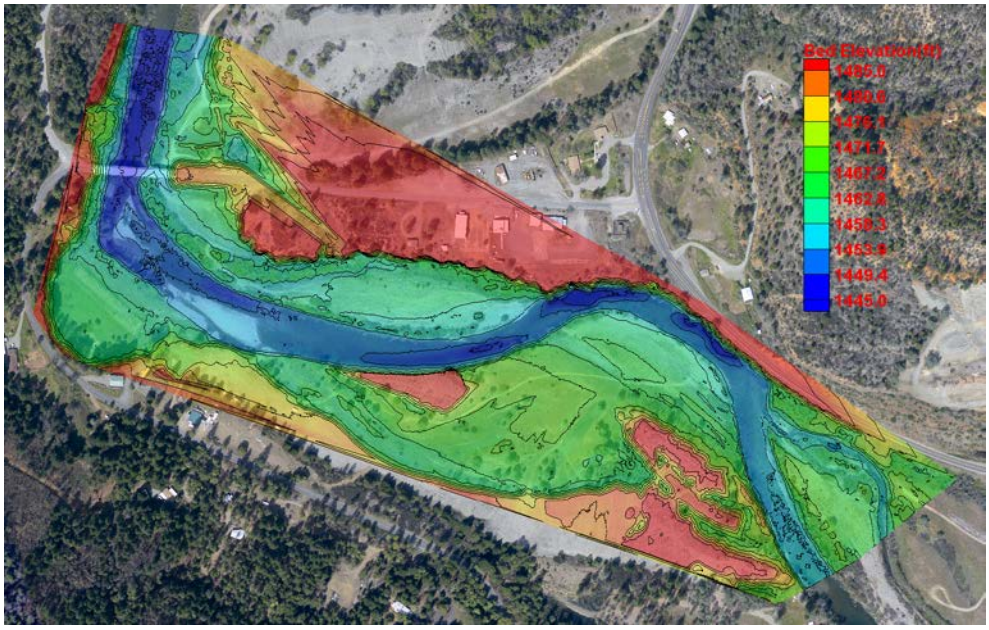

Figure 1. Bed elevation contours based on the 2009 terrain data under the pre-erosion baseline condition (aerial photo was in April 2009)

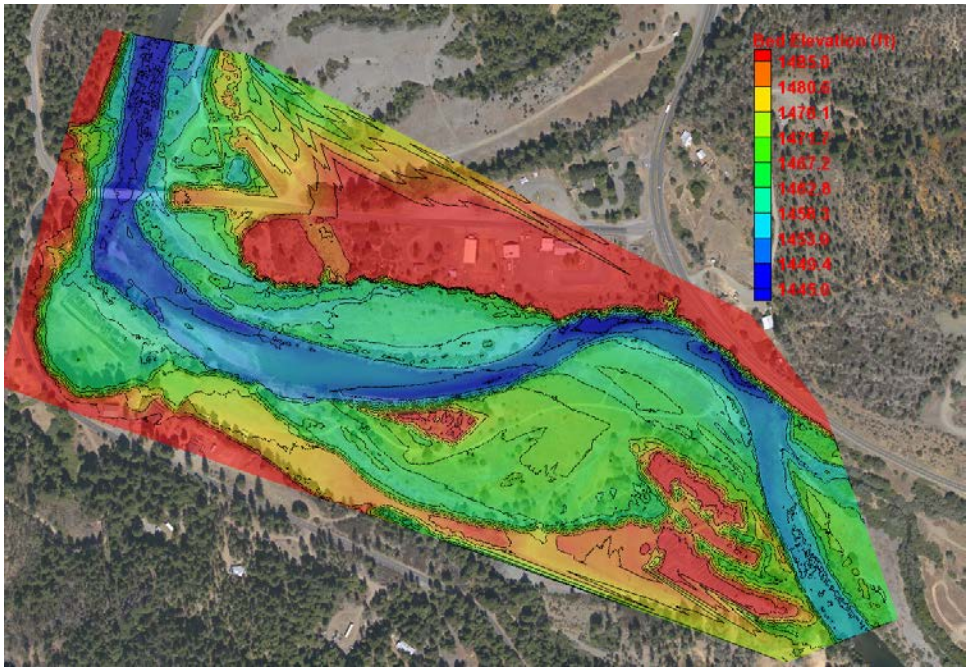

Figure 2. Bed elevation contours based on the 2011 terrain data under the post-erosion condition (aerial photo was in August 2011)

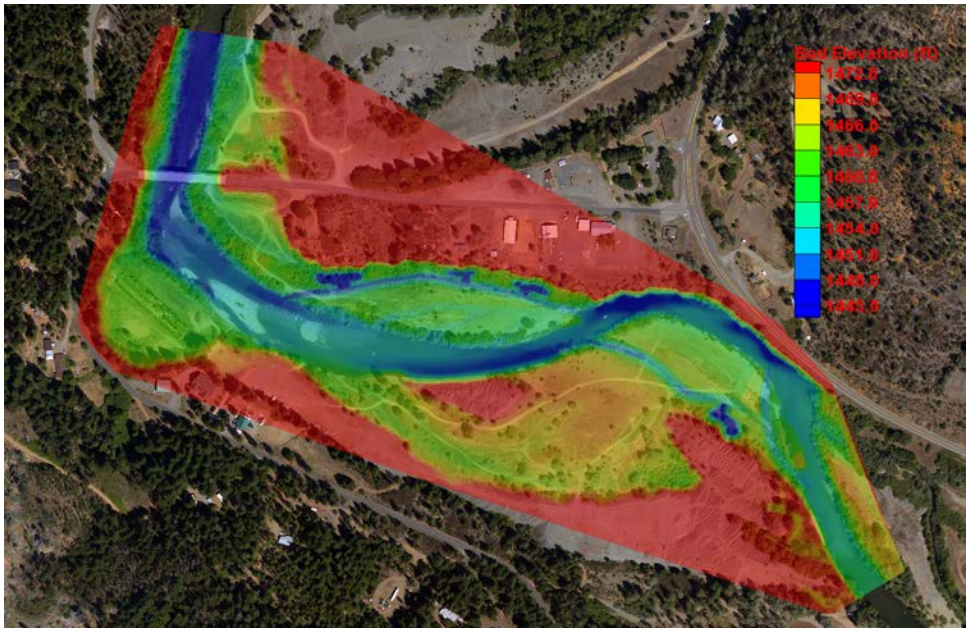

Figure 3. Bed elevation contours based on the design construction condition (aerial photo was in August 2011)

2.2 Bank Data

A total of ten bank locations, named UJC-A through UJC-J, were selected by Cardno ENTRIX for field and BSTEM modeling studies at the UJC site (Cardno ENTRIX, 2012). The ten bank locations are shown in Figure 4. These ten bank locations were used for the preliminary modeling in this study and results are reported in Chapter 4. BSTEM predicted bank sediment loadings at the ten banks locations were estimated by Cardno EXTRIX (2012) and they are shown in Figure 5. Note that the data corresponding to discharges below 4,000 cfs were excluded in the plot since discharges below 4,000 cfs were not simulated for reasons to be discussed later in the report.

Not all ten banks, however, were selected for the coupled morpho-dynamic and bank erosion modeling. For calibration modeling and morphological assessment modeling, only left bank sections from UJC-C to UJC-F were selected. This decision was based on the following analysis. The 2009 and 2011 terrain data was used to estimate the bank retreat at all ten banks. A comparison showed that bank retreats at banks other than UJC-C to UJC-F were relatively small and therefore, they were not modeled for bank retreat in the coupled model. The bank properties used by the coupled models are tabulated in Table 1 through Table 4 for UJC-C to UJC-F; they were obtained from the BSTEM input files of the Cardno ENTRIX (2012) study. Notice that for the sampling site UJC-C to UJC-F, no sample had more than 10% cohesive material, which is typically considered sediment with a particle diameter less than 0.062 mm. Therefore, all the eroding banks are considered non-cohesive.

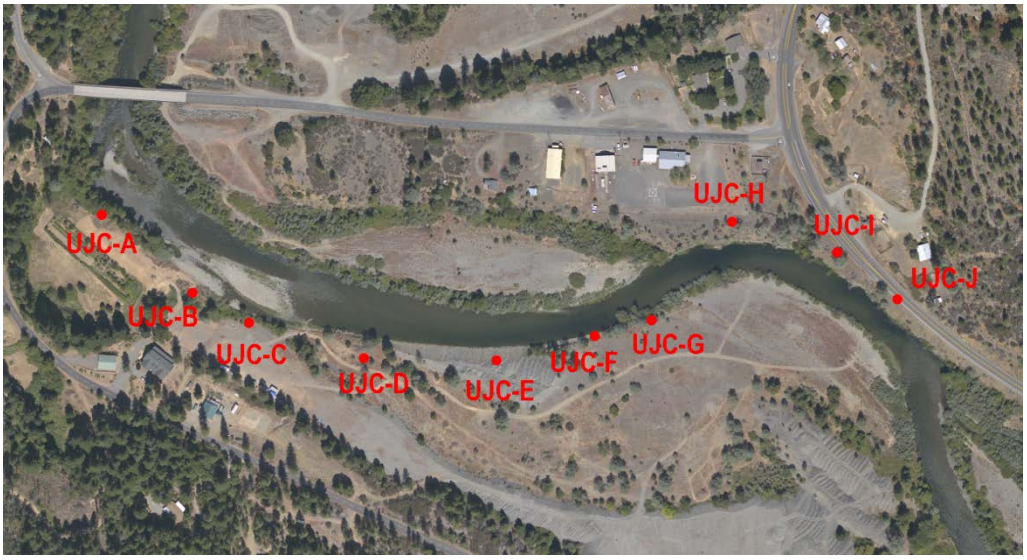

Figure 4. Locations of the ten banks where field survey and BSTEM modeling were carried out by Cardno ENTRIX.

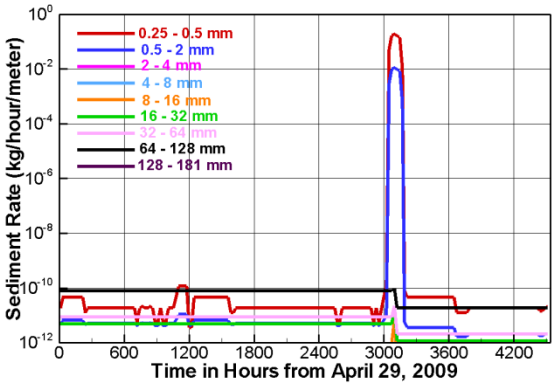

(a) UJC-A

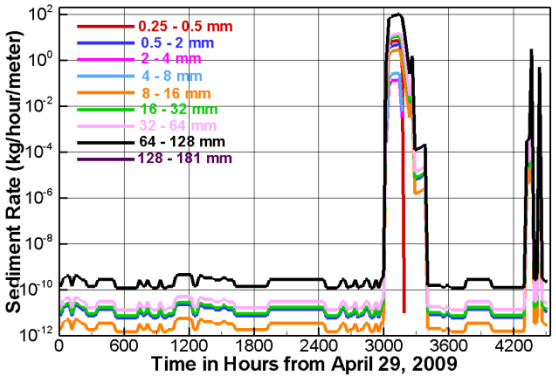

(b) UJC-B

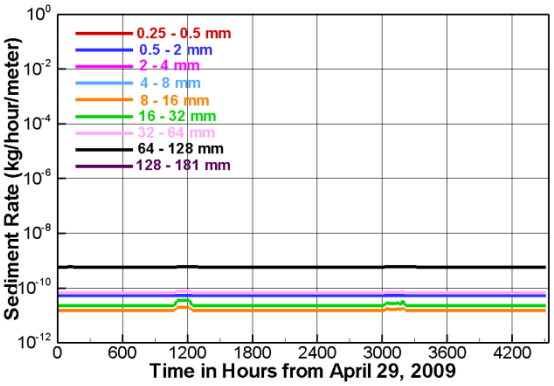

(c) UJC-C

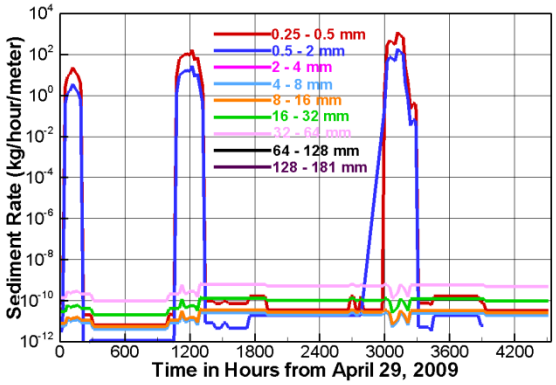

(d) UJC-D

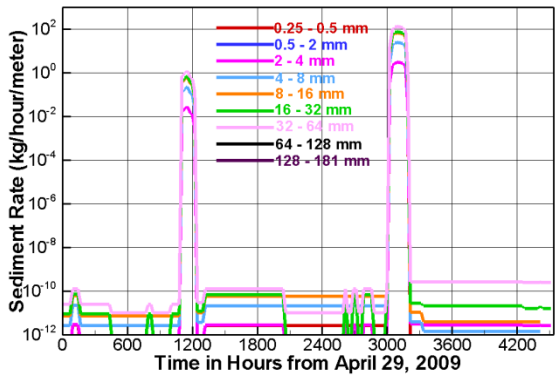

(e) UJC-E

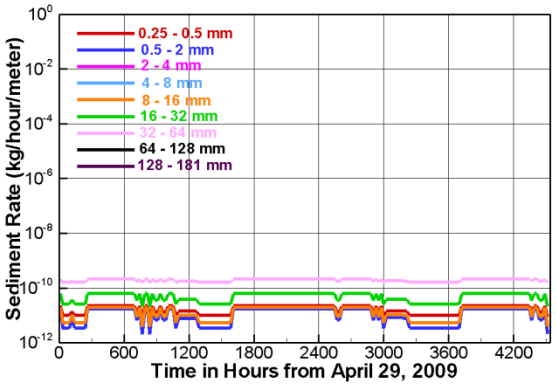

(f) UJC-F

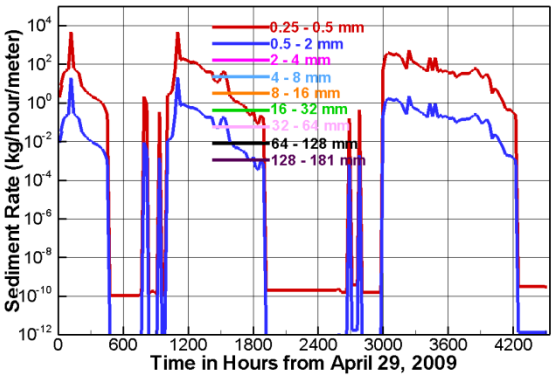

(g) UJC-G

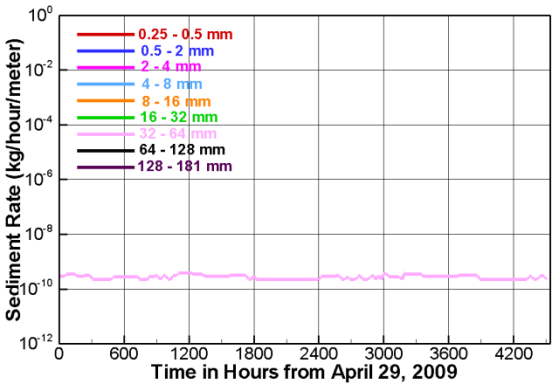

(h) UJC-H

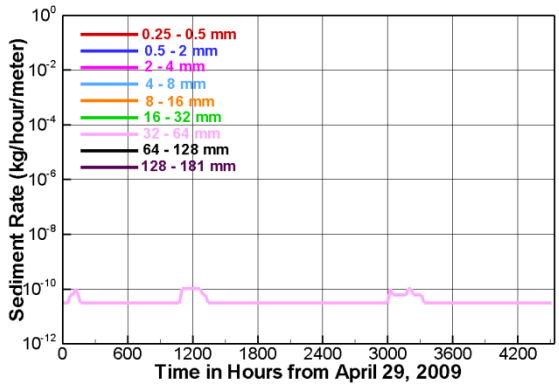

(i) UJC-I

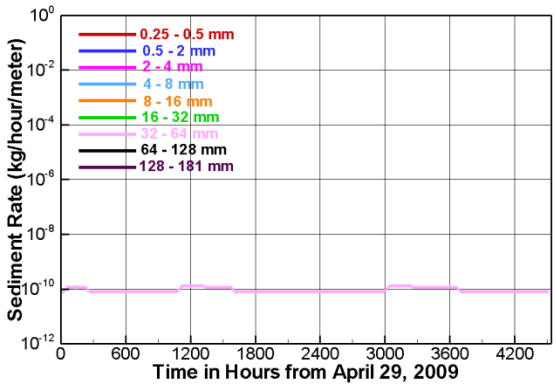

(j) UJC-J

Figure 5. Time series data of BSTEM predicted sediment rates eroded from each of the ten banks (rates plotted are for 9 size classes and over three years from 2009 to 2011); data from Cardno Entrix (2012).

Table 1. Bank properties at UJC-C site from Cardno Entrix (2012)

Bank Layer	Thickness (m)	Critical Shear Stress (Pa)	Erodibility (cm^3/Ns)	Saturated unit weight (kN/m^3)	Friction angle ϕ'	Cohesion c' (kPa)	ϕb	
1	2.6	15.07	0.17	20	36	1	15	
2	2.0	15.07	0.17	20	36	1	15	
3	2.0	15.07	0.17	20	36	1	15	
All three layers have the same following composition (diameter in mm, % finer than)								
<0.5	0.5-1.41	1.41-2	2-4	4-8	8-16	16-32	32-64	>64
0	4	4	4	6	18	50	75	100

Table 2. Bank properties at UJC-D site from Cardno Entrix (2012)

Bank Layer	Thickness (m)	Critical Shear Stress (Pa)	Erodibility (cm^3/Ns)	Saturated unit weight (kN/m^3)	Friction angle ϕ'	Cohesion c' (kPa)	ϕb	
1	0.9	0.71	2.123	18	32	.4	15	
2	0.75	0.71	2.123	18	32	.4	15	
3	0.75	0.71	2.123	18	32	.4	15	
4	0.75	0.71	2.123	18	32	.4	15	
All three layers have the same following composition (diameter in mm, % finer than)								
<.0025	.0025 -.088	.088 -0.25	0.25 -0.354	0.354 -0.5	0.5 -1.41	1.41 -2	2 -4	>4
2.5	6	9.9	27	57	84	94	100	100

Table 3. Bank properties at UJC-E site from Cardno Entrix (2012)

Bank Layer	Thickness (m)	Critical Shear Stress (Pa)	Erodibility (cm^3/Ns)	Saturated unit weight (kN/m^3)	Friction angle ϕ'	Cohesion c' (kPa)	ϕb
1	3	23.81	0.117	20	36	.4	15
2	3	23.81	0.117	20	36	.4	15
3	3	23.81	0.117	20	36	.4	15
4	3	23.81	0.117	20	36	.4	15
All three layers have the same following composition (diameter in mm, % finer than)							
<0.5	0.5-4	4-8	8-16	16-32	32-64	>64	
0	1	2	10	32	57	100	

Table 4. Bank properties at UJC-F site from Cardno Entrix (2012)

Bank Layer	Thickness (m)	Critical Shear Stress (Pa)	Erodibility (cm^3/Ns)	Saturated unit weight (kN/m^3)	Friction angle ϕ'	Cohesion c' (kPa)	ϕb
1	0.6	7.78	0.294	20	36	0	15
2	1.95	7.78	0.294	20	36	0	15
3	1.95	20.9	0.13	20	36	0	15
4	1.5	20.9	0.13	20	36	0	15
5	1.5	75.33	0.045	20	36	0	15

Layer 1 & 2 composition (diameter in mm, % finer than)									
<.002	.002-.063	.063-.354	.354-.5	0.5-1.41	1.41-2	2-16	16-32	32-64	>64
0	1.19	6.19	14.23	23.21	31.24	46	62	83	100

Layer 3 & 4 composition (diameter in mm, % finer than)									
<.002	.002-.063	.063-.354	.354-.5	0.5-1.41	1.41-2	2-16	16-32	32-64	>64
0	0.55	3.48	6.73	11.15	15.53	25	35	62	100

Layer 5 composition (diameter in mm, % finer than)				
<0.5	0.5-16	16-32	32-64	>64
0	4	5	14	100

3 Numerical Model Details and Steps

3.1 SRH-2D Model Description

SRH-2D version 3, Sedimentation and River Hydraulics – Two-Dimensional, was used for the current modeling study. SRH-2D was a 2D depth-averaged hydraulic and sediment transport mobile-bed model for river systems. It was developed at the Technical Service Center, Bureau of Reclamation. The hydraulic flow model, documented by Lai (2008; 2010), has been widely used by internal and external users. The sediment transport mobile-bed model, used to predict stream bed vertical change, is still under development. It, however, has been applied to a wide range of projects at Reclamation since 2008. The mobile-bed model theory and selected results may be found in Greimann et al. (2008), Lai and Randle (2007), Lai and Greimann (2008; 2010) and Lai et al. (2011). At present, a beta-version has been distributed to selected users.

The robustness and reliability of SRH-2D have been proven with a wide range of Reclamation projects as well as with studies at external institutions. Detailed technical information of SRH-2D and selected application cases may be downloaded from the following Reclamation website: http://www.usbr.gov/pmts/sediment/. Some of the unique features of SRH-2D have been discussed by Lai (2008). A primary feature is the use of a flexible mesh. The arbitrarily shaped element method of Lai et al. (2003) is adopted for geometry representation. This essentially allows the use of most existing meshes available: structured quadrilateral mesh, purely triangular finite element mesh, Cartesian mesh, or hybrid mesh. Our experience showed that the hybrid mesh, in which a combination of quadrilateral meshes along main channel and triangular meshes in the remaining zones was used, would be most flexible. It often leads to increased accuracy and efficiency. Other important features include the relatively stable numerical algorithms used with very few stability-ensuring parameters and ease of use of the model.

Major modeling capabilities of SRH-2D are as follows:

- 2D depth-averaged governing equations with the dynamic wave (shallow water) approximation for flow hydraulics;
- An implicit solution scheme for time advancement;
- Unstructured meshes with arbitrary mesh cell shapes. In most applications, a combination of quadrilateral and triangular meshes is recommended;
- Steady or unsteady flows;
- Subcritical, supercritical or transcritical flow regimes;
- Time-accurate, non-equilibrium modeling of sediment transport;
- Multi-size-class sediment transports with bed sorting and armoring;

- A unified formulation for suspended load, bedload and mixed load;
- Effects of gravity and secondary flows;
- Non-cohesive or cohesive sediments; and
- Coupled mobile-bed and bank erosion modeling.

SRH-2D is a 2D model; it is particularly useful for problems where 2D effects are important. Examples include flows with in-stream structures such as weirs, diversion dams, release gates, coffer dams, etc.; bends and point bars; perched rivers; and multi-threaded streams. 2D models may also be needed if some flow features are important such as flow recirculation and eddies, lateral variations, overtopping over banks and levees, differential flow shears on river banks, and interactions between the main channel, vegetated areas and floodplains. Some of the scenarios listed above may be modeled by 1D models. However, additional empirical sub-models need to be supplemented and extra calibrations must be carried out with unknown uncertainties.

The coupled morpho-dynamic and bank erosion model is still undergoing research and development. Readers may refer to the papers of Lai (2012a; 2012b) for the current status of the model.

3.2 Model Setup Details

SRH-2D modeling, in general, includes the following steps:

(1) Selection of the solution domain;
(2) Mesh generation for the solution domain and definition of boundary conditions;
(3) Topography, flow roughness, and bed sediment gradation representation;
(4) Model calibration; and
(5) Model applications.

The first three steps are discussed below; the remaining steps are reported in later chapters.

3.2.1 Scenarios Simulated

Three sets of modeling were carried out.

The first was the “preliminary modeling” (PM) in which the terrains of the 2011 post-erosion condition (PC) and the 2012 design construction (DC) condition were used as the initial bathymetry and runs without and with the BSTEM predicted bank sediment loadings were carried out. Simulation was carried out with a three-year hydrograph from 2009 to 2011. The PM runs were intended to provide a quick assessment of the UJC site before the time-intensive, coupled modeling could be carried out. The PM results are presented in Chapter 4 of this report.

The second was the calibration study under the 2009 "pre-erosion baseline" (PB) condition using the coupled morpho-dynamic and bank erosion model. The linear retreat bank erosion model suitable for non-cohesive banks was adopted. The PB cases used the 2009 terrain as the initial bathymetry and were simulated for a three-year hydrograph from 2009 to 2011. The predicted 2011 results by the PB runs were compared to the measured 2011 terrain data for model calibration and verification. The PB results are presented in Chapter 5 of this report.

The third was the "morphologic assessment" (MA) modeling in order to assess the design construction impact on stream morphology. Two conditions were modeled: the 2011 "post-erosion condition" (PC) and the 2012 "design construction" (DC) condition. The PC modeling runs utilized the 2011 terrain as the initial bathymetry while the DC runs started with an initial bathymetry according to the design construction of the river rehabilitation project at the UJC site. The morphological changes of the study site under PC and DC conditions were simulated with the same three-year hydrograph as the PB condition. Since the design construction terrain was close to the 2011 terrain and all model parameters were the same, a comparison of the PC and DC modeling results provided the necessary data to understand the impact of the design construction on channel morphology. Note that only a 3-year hydrograph was used in the assessment and long-term equilibrium channel form was not attempted. The MA results are presented in Chapter 6 of this report.

3.2.2 Solution Domain, Mesh and Zonal Representation

A 2D analysis begins by defining a solution domain and then generating a mesh that covers the domain. The solution domain may be determined according to the project study questions, river reach characteristics of interest, and upstream and downstream channel forms. The domain may also be constrained by available survey data due to high costs of bathymetric and topographic surveys. In this study, the solution domain was limited by the available terrain data. The final solution domain selected is displayed in Figure 6. The solution domain encompassed about 4,000 ft in channel length and an average of 700 ft in width.

Meshes were generated using the Surface-water Modeling System software (SMS). The following website link provides the information about SMS: http://www.aquaveo.com. Additionally, SRH-2D manual (Lai, 2008) may be used for how to generate an appropriate 2D mesh. Three meshes were generated corresponding to the three modeling conditions (PM, PB and MA). The same mesh was used with the PC and DC scenarios for the PM and MA modeling runs so that the differences of the model results between the two were mainly due to the modifications introduced by the design construction. Herein, two meshes are called the same if the horizontal coordinates of all mesh points are identical though the bed elevation of mesh points may be different. Three meshes, with their horizontal mesh point displayed, are shown in Figure 6 through Figure 8. They consisted of mixed quadrilaterals and triangles with a total of 17,605, 18,414 and 19,119 mesh cells, respectively, for the PM, PB and MA conditions. There were three initial terrains for all modeling runs: the 2009 pre-erosion, the

2011 post-erosion, and 2012 design construction scenarios. 3D perspective views of the three initial terrains represented by the meshes are shown in Figure 9 through Figure 11.

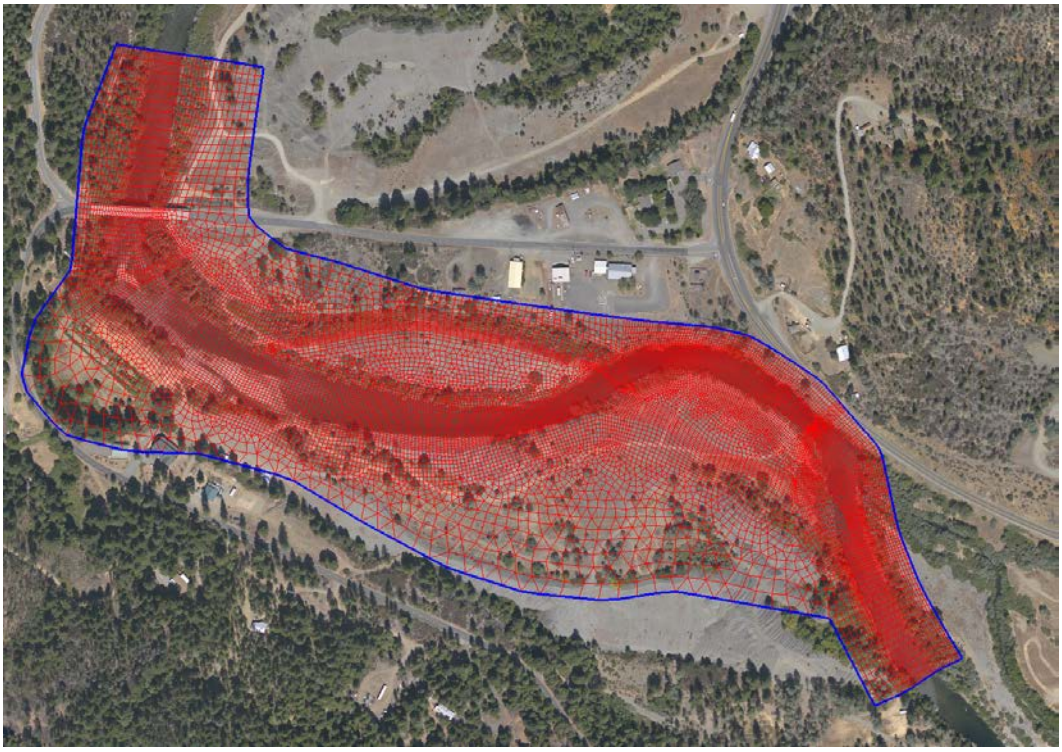

Figure 6. Solution domain (blue) and the mesh (red) for the PM (preliminary modeling) condition modeling (aerial photo was in August 2011).

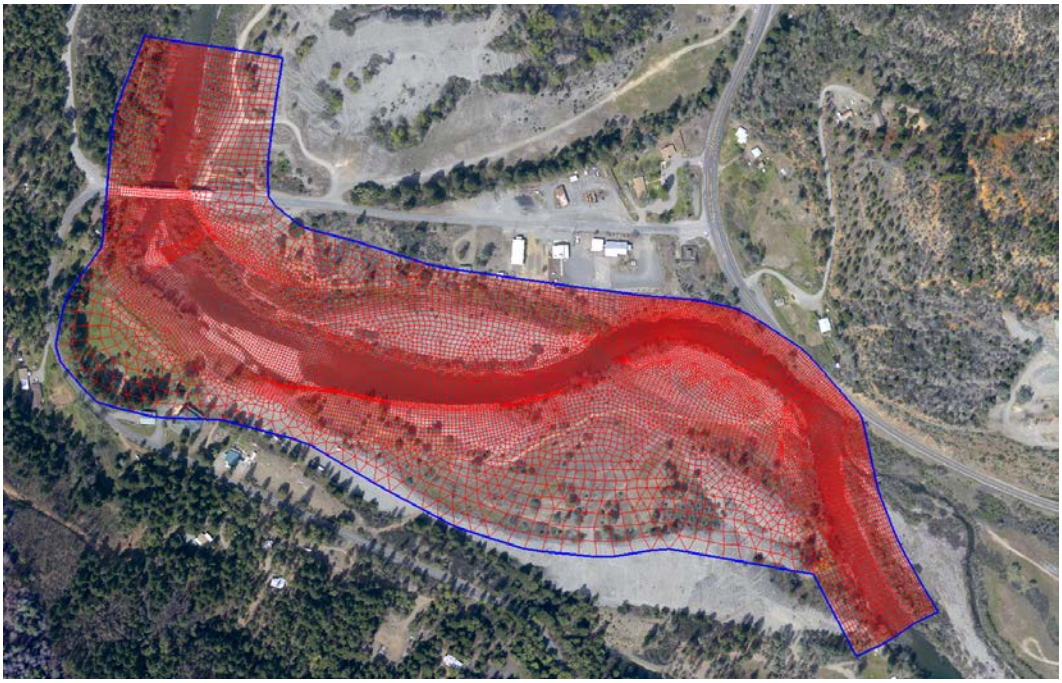

Figure 7. Solution domain (blue) and the mesh (red) for the PB (pre-erosion baseline) condition modeling (aerial photo was in April 2009).

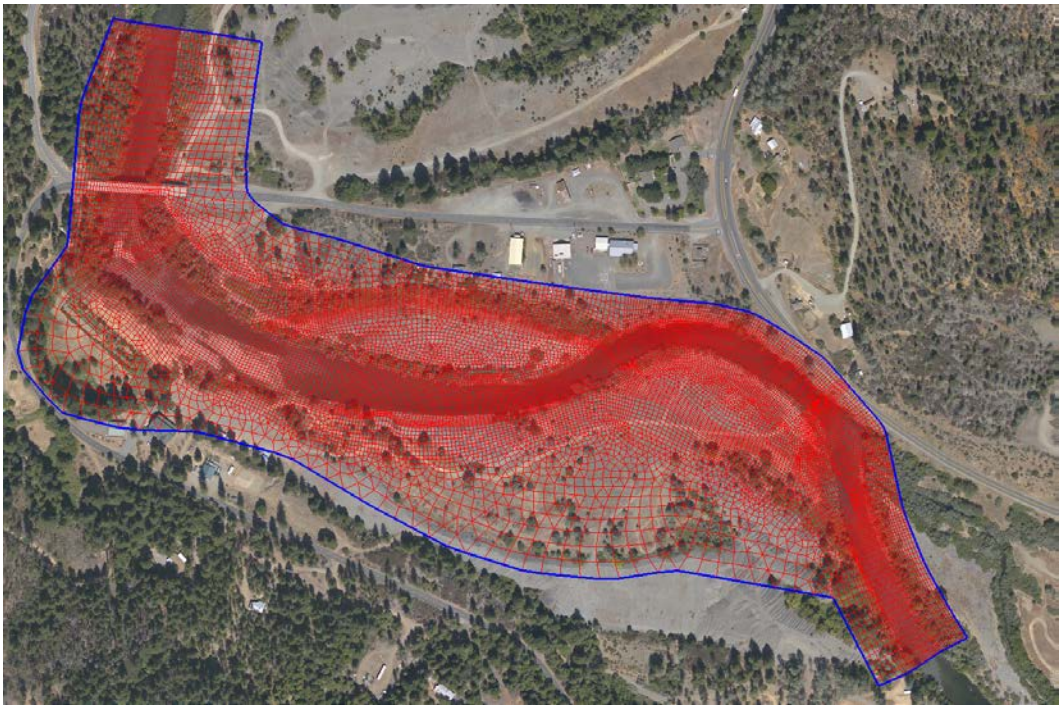

Figure 8. Solution domain (blue) and the mesh (red) for the MA (morphologic assessment) condition modeling (aerial photo was in August 2011).

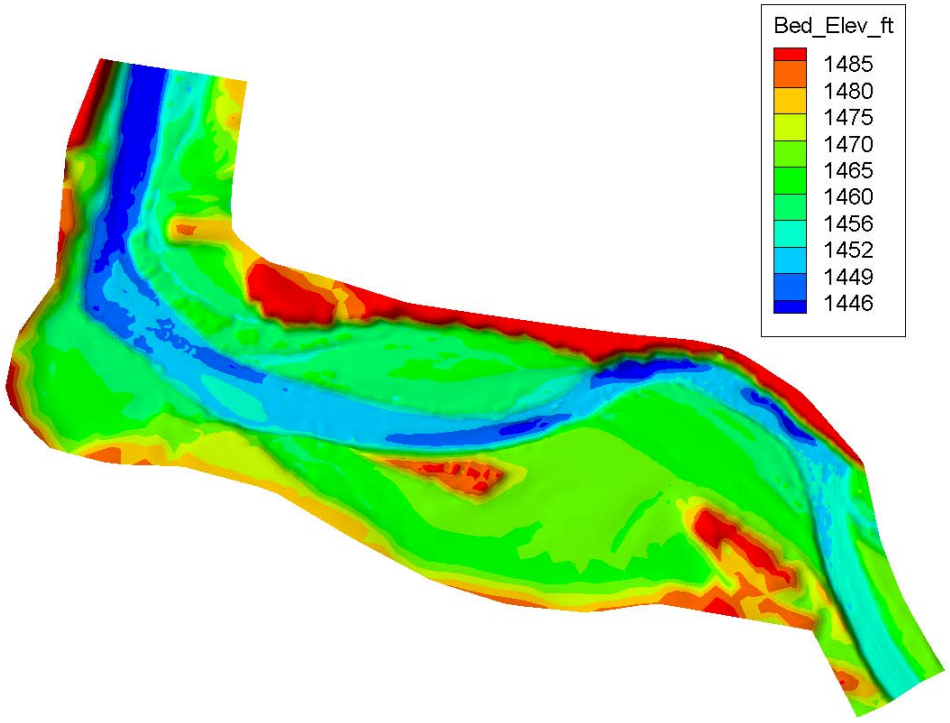

Figure 9. Bed elevation contours for the 2009 pre-erosion baseline terrain.

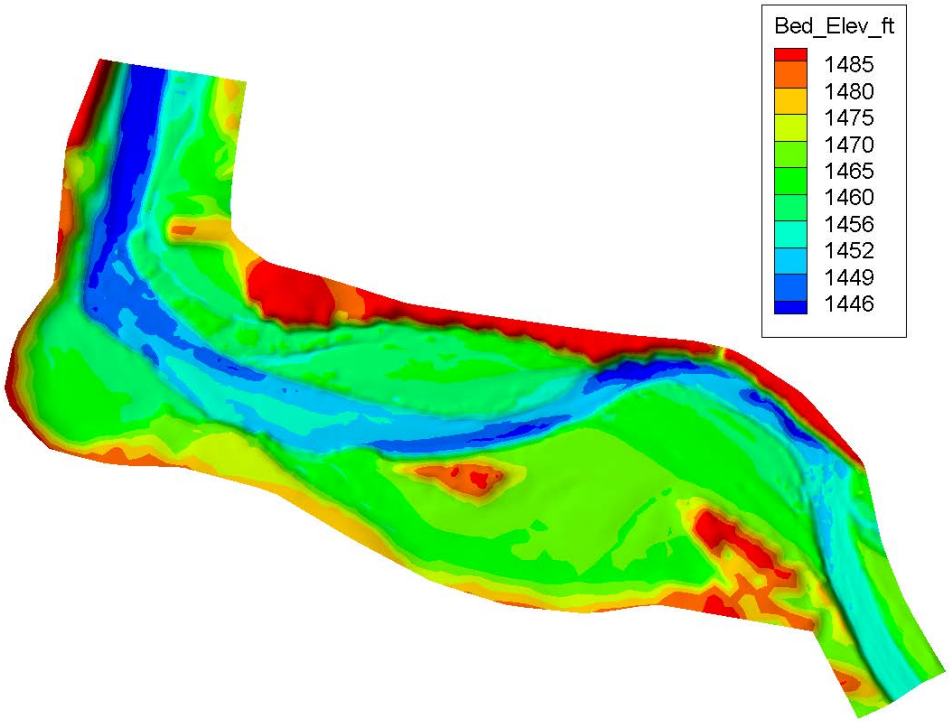

Figure 10. Bed elevation contours for the 2011 post-erosion terrain.

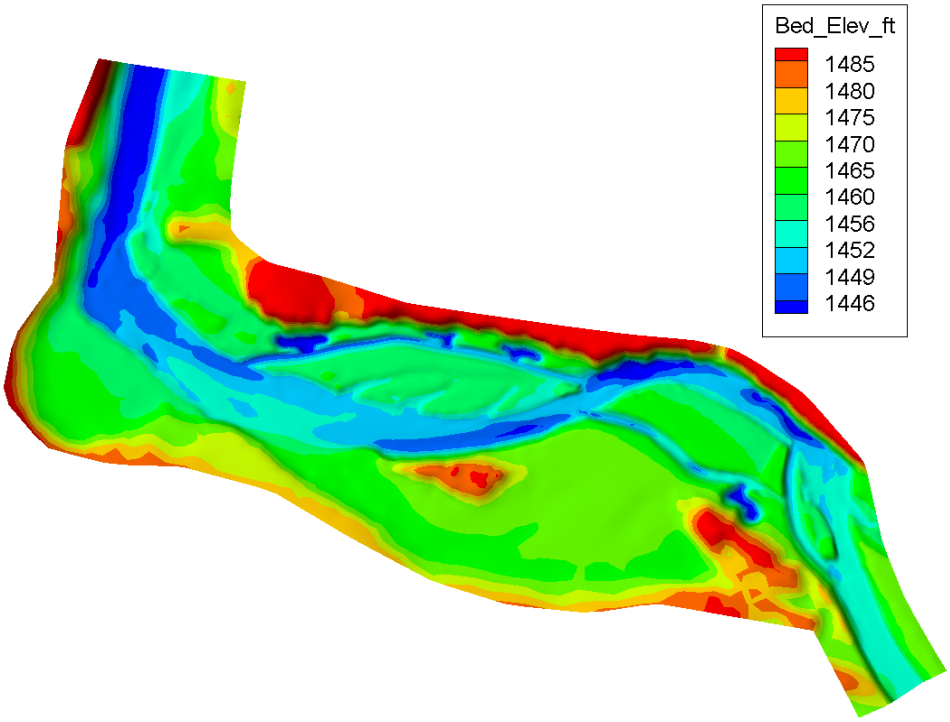

Figure 11. Bed elevation contours for the 2012 design construction terrain.

Flow resistance was computed with the Manning's roughness equation in which the Manning's coefficient (*n*) was used as one of the model inputs. The Manning's coefficient may be estimated from the field, based on previous studies on the same or similar rivers, or calibrated using the measured water surface elevation data. In this study, it was estimated from the previous studies on the Trinity River. The solution domain was divided into three zones as shown in Figure 12 through Figure 14 for the three terrain scenarios. The Manning's coefficient for each zone was assigned with the following values: 0.035 for the main channel and the bare floodplain, and 0.085 for the vegetation zone.

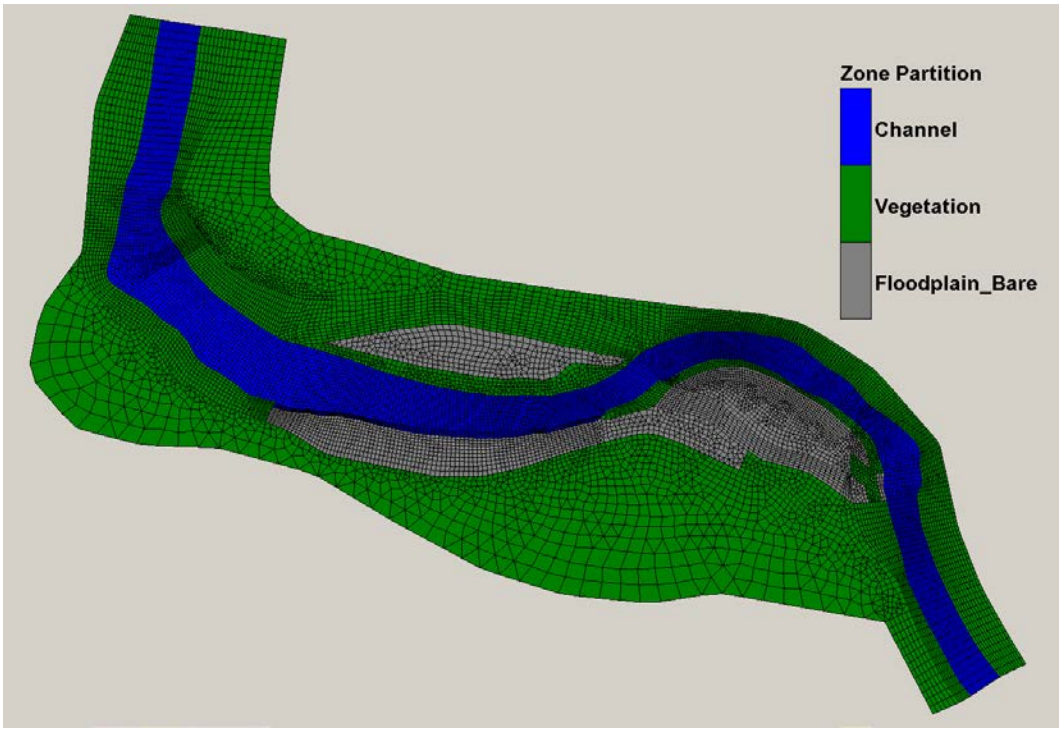

Figure 12. Zonal partition of the solution domain for both roughness assignment and bed gradation representation for the PB (pre-erosion baseline) condition.

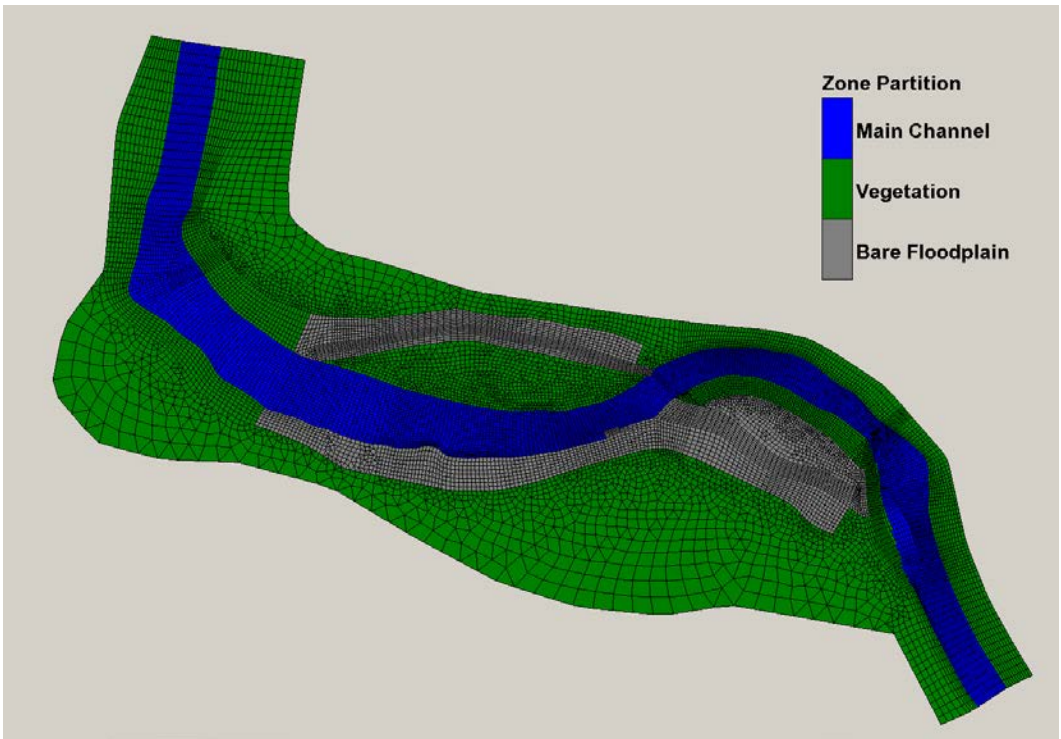

Figure 13. Zonal partition of the solution domain for both roughness assignment and bed gradation representation for the PC (post-erosion) scenario runs.

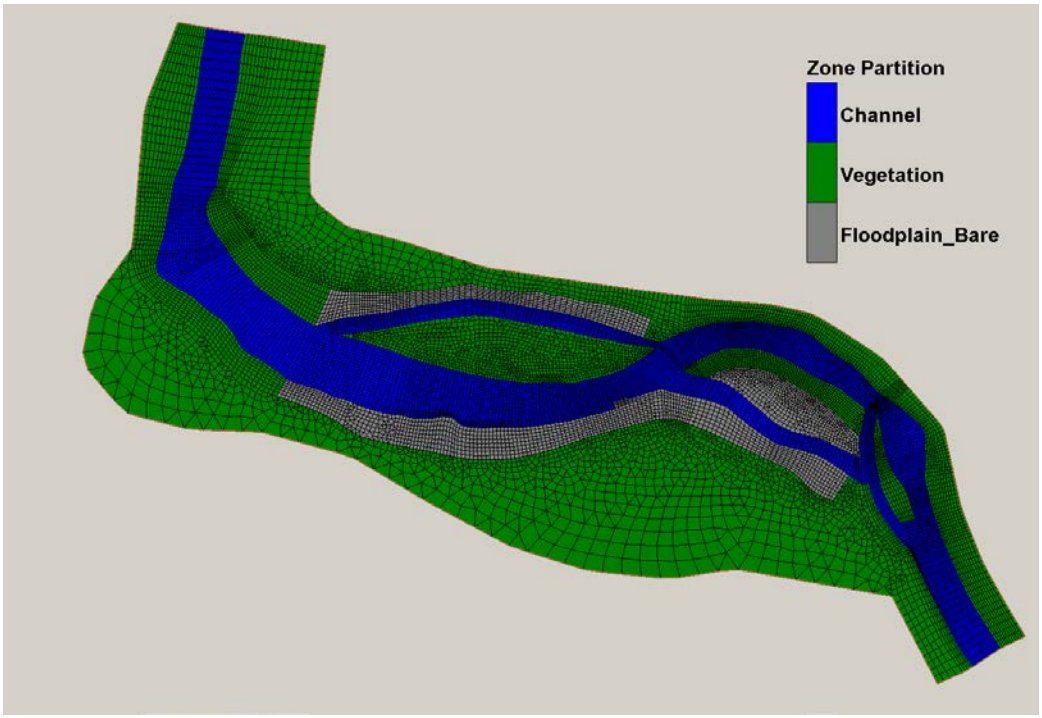

Figure 14. Zonal partition of the solution domain for both roughness assignment and bed gradation representation for the DC (design construction) scenario runs.

The bed sediment gradation over the solution domain was also needed for the mobile bed vertical erosion modeling. The bed gradation was represented by the same zonal partition in Figure 12 through Figure 14. The bed sediment in the main channel was divided into two layers. The top layer had about 0.65 ft thickness while the bottom layer had infinite thickness. The bed gradations of each layer are plotted in Figure 15. The gradations were almost the same for the two layers with a medium diameter (d_{50}) of about 29 mm. The bare floodplain was assumed to have the uniform sediment gradation the same as the bottom layer of the main channel. In the vegetated zones, only deposition was allowed and therefore, no bed gradation was needed by the model.

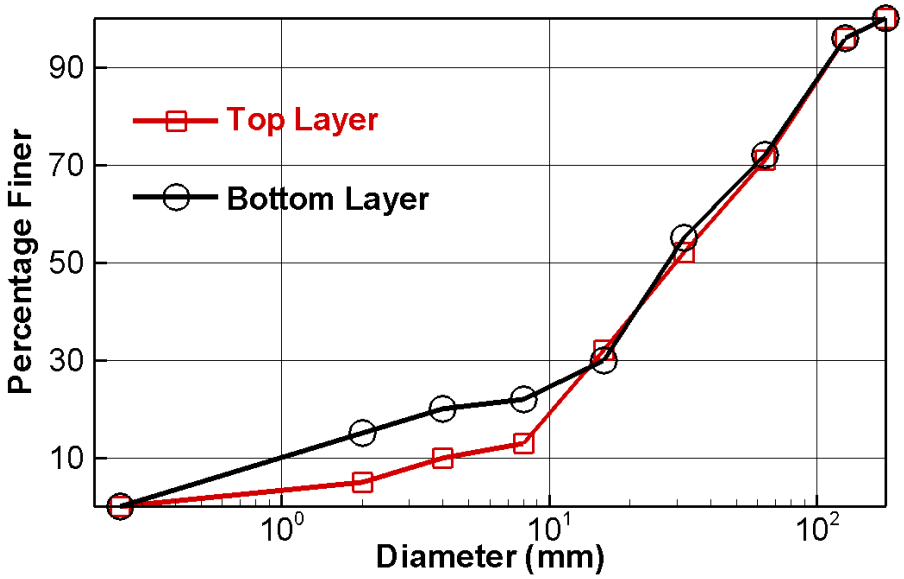

Figure 15. Bed sediment gradation distribution of the study site.

3.2.3 Boundary Conditions and Other Model Inputs

Time-accurate unsteady simulations were carried out using the hydrograph from April 29, 2009 to September 3, 2011 (USGS gaging station 11526250) that covered three spring runoffs. The daily flow hydrograph is shown in Figure 16. The hydrograph was used as the upstream flow boundary condition for all model runs. Only discharges above a pre-selected value were used for mobile-bed modeling. Eliminating low flows was done for two reasons: (1) only large flows mobilized stream bed and changed stream morphology; and (2) computing time can be reduced significantly by ignoring the smaller flows since the sediment transport simulations were very time intensive. The cutoff discharge for the PB runs was 2,000 cfs while it was 4,000 cfs for the PM and MA runs. Use of the 4,000 cfs cutoff might be too high but it was justified for the present study since the PC and DC scenario runs under the PM and MA conditions were used for relative comparisons so that the project impact on stream morphology might be obtained. The time series discharges after removal of flows below the cutoff discharges are displayed in Figure 17. The total simulated time period was reduced to about 22% and 6.7% of the original time, respectively, with the 2,000 cfs and 4,000 cfs cutoff discharges. It is cautioned that potential suspended sediment deposition in the side channel or floodplains may be under-predicted by excluding the flows lower than the cutoff discharge.

The cutoff discharge was important for the PB condition runs and its effect on channel morphology might be evaluated by computing the Shields parameter distribution in the stream. With a 2,000 cfs discharge, the Shields parameter in the stream was computed by SRH-2D and shown in Figure 18. The Shields parameter was defined by:

$$\theta = \frac{\tau_b}{g(\rho_s - \rho_w)d_{ref}} \quad (1)$$

where τ_b was the model predicted bed shear stress, ρ_w and ρ_s were water and sediment densities, respectively, g was gravity acceleration, and d_{ref} was the reference diameter (29 mm). The results suggested that a flow of 2,000 cfs might mobilize sediments in only few areas but the changes in morphology were expected to be small.

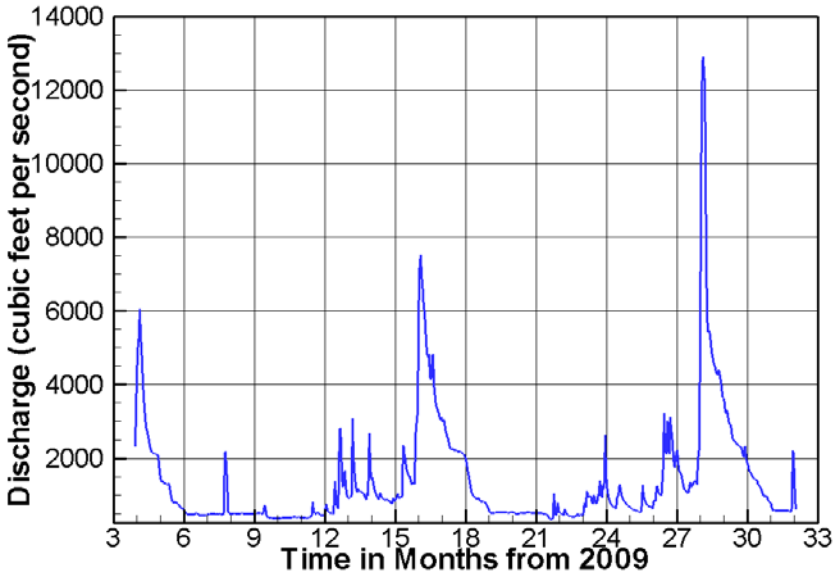

Figure 16. Daily flow discharges from April 29, 2009 to September 3, 2011 at the Upper Junction City site.

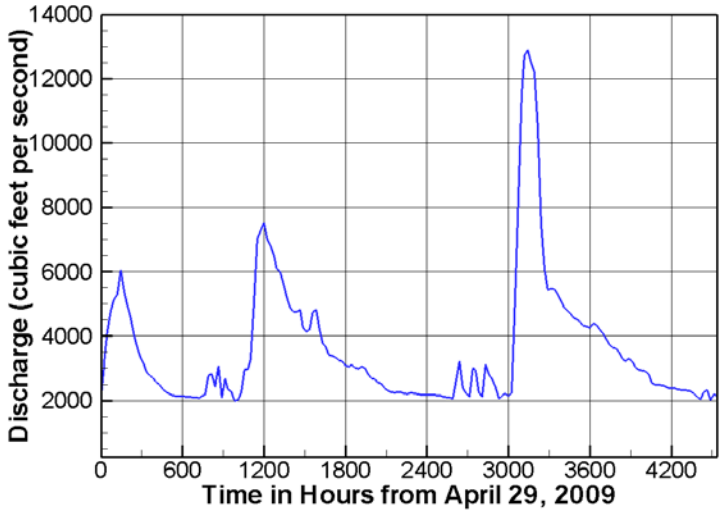

(a) Cutoff discharge of 2,000 cfs was applied

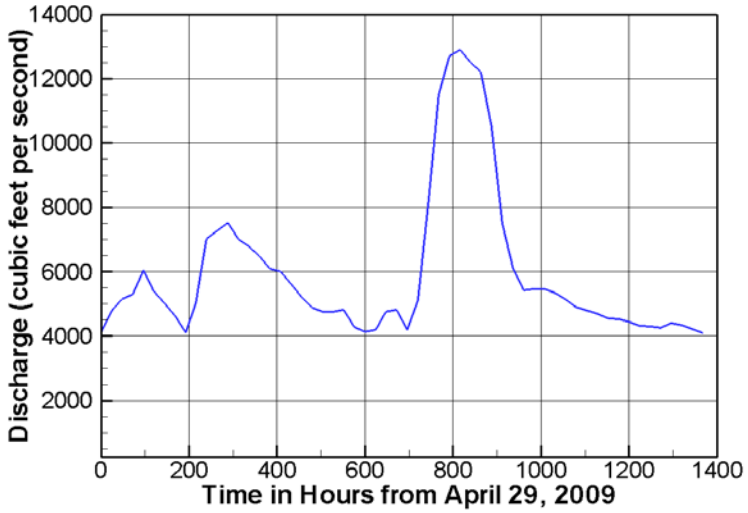

(b) Cutoff discharge of 4,000 cfs was applied

Figure 17. Daily flow discharges at the Upper Junction City site after removal of smaller discharges below the cutoff values.

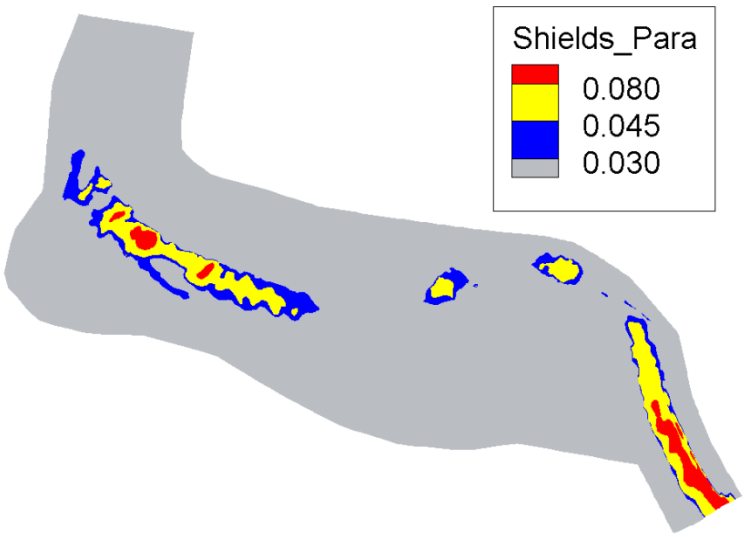

Figure 18. Computed Shields parameter distribution in the stream with a constant flow of 2,000 cfs and a reference sediment diameter of 29 mm.

Sediment load was needed as another upstream boundary condition. In this study, the sediment rating curves developed by TRRP, based on the 2006-2007 sediment data at the Douglas City site of the Trinity River, were used. They are plotted in Figure 19. It is seen that the two largest size classes (above 64 mm) had higher sediment rates than those of the smaller ones (2-32 mm range) when the flow was above 7,000 cfs.

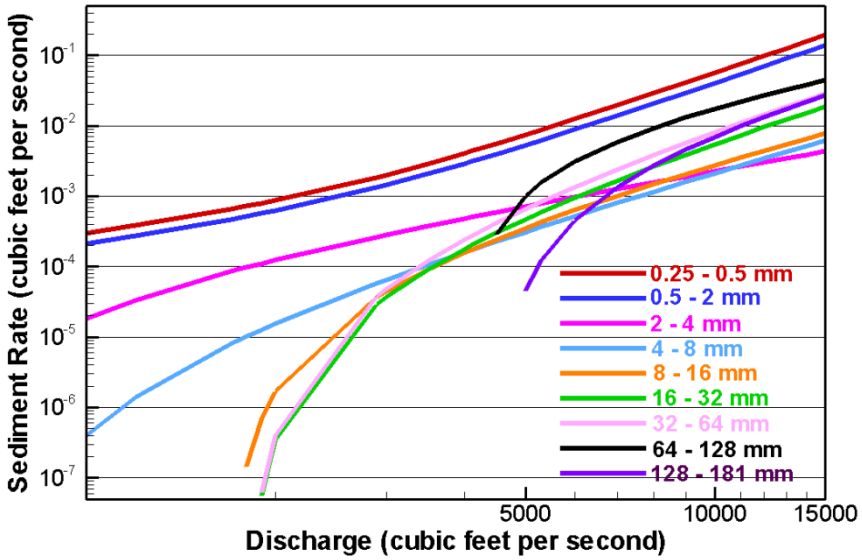

Figure 19. Sediment rate rating curves for various sediment size classes used as the upstream sediment load.

Water surface elevation (stage) was needed as the downstream boundary condition. A stage-discharge rating curve was generated using HEC-RAS model by TRRP and used as the boundary condition (see Figure 20).

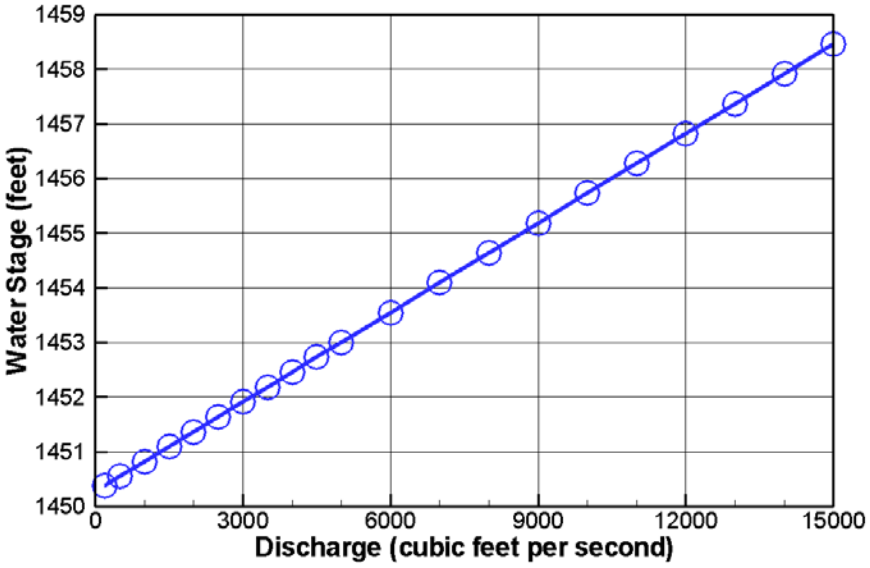

Figure 20. Stage-discharge rating curve used as the downstream boundary condition.

A total of nine sediment size classes were used to represent bed materials as tabulated in Table 5. The geometric mean is used by SRH-2D for each size class.

Most model runs selected the sediment transport capacity equation developed by Gaeuman et al. (2009), named Trinity capacity equation, unless it is stated otherwise in this report. The Trinity capacity equation for a sediment size class *k* may be expressed as:

$$\frac{q_{t,k}^{*} g(s-1)}{(\tau_b / \rho_w)^{1.5}} = p_{ak} G(\phi_k); \qquad \phi_k = \frac{\theta_k}{\theta_r}\left(\frac{d_k}{d_{50}}\right)^{\alpha_k} \tag{2}$$

In the above, $q_{t,k}^{*}$ is the volumetric sediment transport rate per unit width, p_{ak} is the volumetric fraction of sediment size class *k* on the bed surface, $s = \rho_S / \rho_w$, ρ_w and ρ_S are the water and sediment density, respectively, *g* is the gravitational acceleration, τ_b is bed shear stress, $\theta_k = \tau_b / [\rho_w g(s-1) d_k]$ is Shield's parameter of sediment size class *k*; θ_r is the reference Shield's parameter, d_k is diameter of sediment size class *k*, and d_{50} is the median diameter of the sediment mixture in bed. The function in the transport equation is expressed as:

$$G(\phi) = \begin{cases} 14.0(1 - 0.894/\phi^{0.5})^{4.5} & \phi \geq 1.35 \\ 0.002\phi^{7.5} & \phi < 1.35 \end{cases} \tag{3}$$

Two parameters must be defined to apply the above equation: θ_r and α_k. The parameter θ_r is a reference value above which sediment is mobilized and α_k is the exposure or hiding factor to account for reduction in critical shear stress for larger particles and increase in critical shear stress for smaller particles. The standard Trinity equation used the following values in SRH-2D:

$$\theta_r = 0.021 + 0.0155\exp(-20F_s) \tag{4a}$$

$$\alpha_k = 1 - \frac{0.7}{1 + \exp(1.9 - d_k / 3d_{50})} \tag{4b}$$

where F_s is the fraction of sand on the bed surface (the cutoff diameter of the "sand" may range from 1 to 4 mm). In this study, a constant reference value $\theta_r = 0.035$ was used. As a comparison, the Wilcock-Crowe (2003) capacity equation used the following default values:

$$\theta_r = 0.021 + 0.015\exp(-20F_s) \tag{5a}$$

$$\alpha_k = 1 - \frac{0.67}{1 + \exp(1.5 - d_k / d_{50})} \tag{5b}$$

Table 5. Size ranges of all sediment size classes

Sediment Size Class	Size Range (mm)
1	0.25 to 0.5
2	0.5 to 2
3	2 to 4
4	4 to 8
5	8 to 16
6	16 to 32
7	32 to 64
8	64 to 128
9	128 to 181

Other model inputs included the following. The time step was 5 seconds that was mainly for numerical stability control. The active layer thickness was chosen to be 0.15 ft, about five times d_{50} and 1.5 times d_{90}. The adaptation length of the bedload was one of the more important input parameters. By default, a constant bedload adaptation length of 80 meters was used unless it is stated otherwise in the report.

3.2.4 Bank Erosion Input Parameters

Additional input parameters were related to the bank properties necessary for a coupled morpho-dynamic and bank erosion modeling. A section of the river left bank was selected for bank retreat modeling and it is shown in Figure 21. The bank section encompassed banks UJC-C to UJC-F (see Figure 4) according to the naming in the study of Cardno ENTRIX (2012). Bank properties of the four banks (UJC-C to UJC-F), as reported by Cardno ENTRIX (2012), were used and it has been discussed in Section 2.2. The time step for the bank erosion model was independent of SRH-2D in the stream; it was six hours for all coupled modeling runs.

The selected bank section was represented by a total of sixteen cross sections in the 2D mesh as shown in Figure 21. Each of the sixteen was simulated using the bank erosion model for its retreat. An analysis of the field data and BSTEM study results reported in Cardno ENTRIX (2012) showed that the selected bank section consisted of essentially uniform and non-cohesive materials (see Section 2.2). It was, therefore, decided that the non-cohesive linear retreat bank erosion model was adopted for the modeling instead of the more sophisticated BSTEM model that was more suitable for the multi-layer cohesive banks. For a detailed discussion of the linear retreat and BSTEM bank erosion models implemented in SRH-2D, readers are referred to Lai et al. (2012a; 2012b). With the linear retreat bank erosion model, the key input parameters were critical shear stress and erodibility at each bank, and the bank failure was determined by the angle of repose approach.

Eroded sediments from banks were added back to the stream in the current SRH-2D implementation of the coupled modeling. However, a user has to supply the

information of how the eroded bank sediments are distributed spatially in the stream. For the current study, user-supplied deposition zones were generated as shown in Figure 23. It was implemented as follows: for deposition zone *i*, for example, eroded bank sediments from all banks encompassed by zone *i* were added to mesh cells in zone *i* uniformly. In addition, SRH-2D allowed the mesh to move and deform along with retreating banks. Users were required to specify the mesh zone in which the mesh would be deformed. In this study, the moving mesh zone was specified as shown in Figure 24.

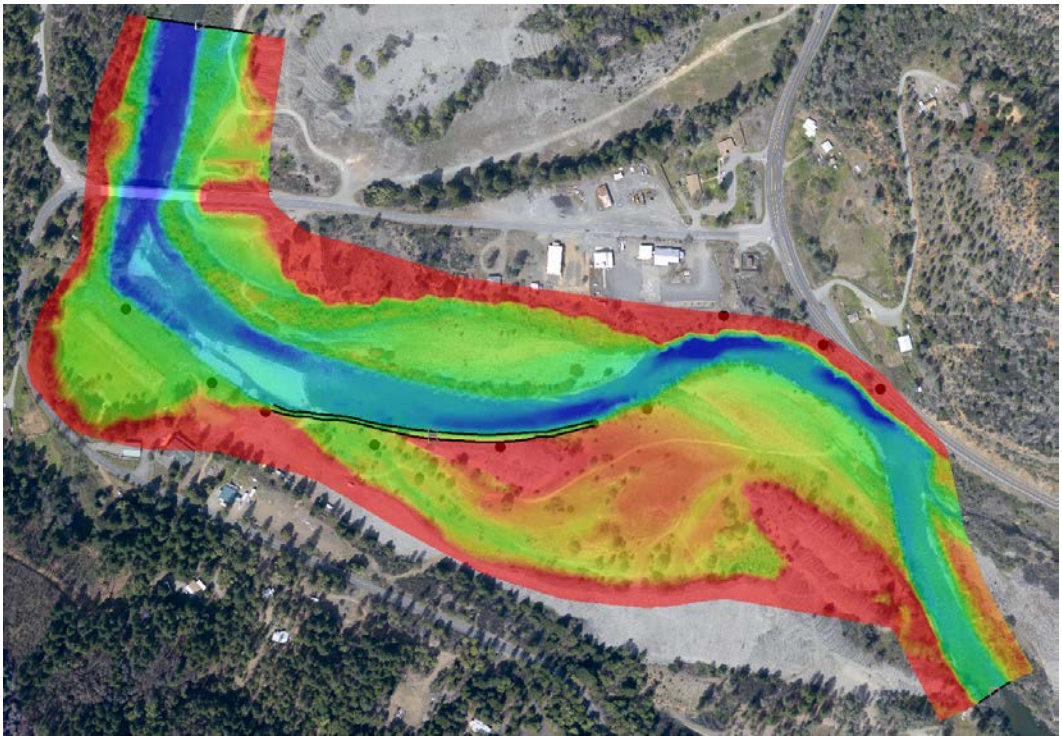

(a) Overall View

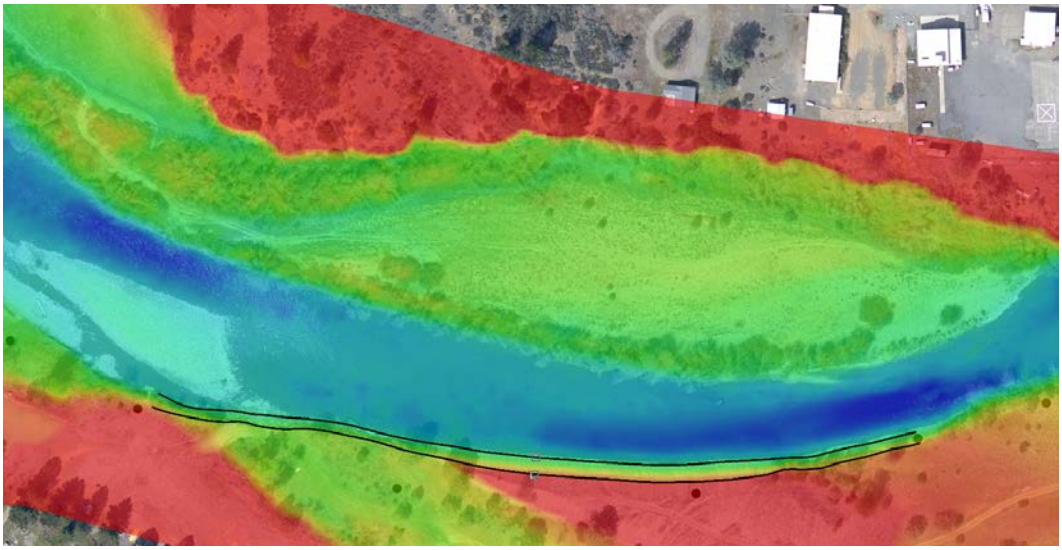

(b) Zoom-In View

Figure 21. The bank section selected for bank erosion modeling under the PB (pre-erosion baseline) condition; black lines show the bank toe and top and the background aerial photo was in April 2009.

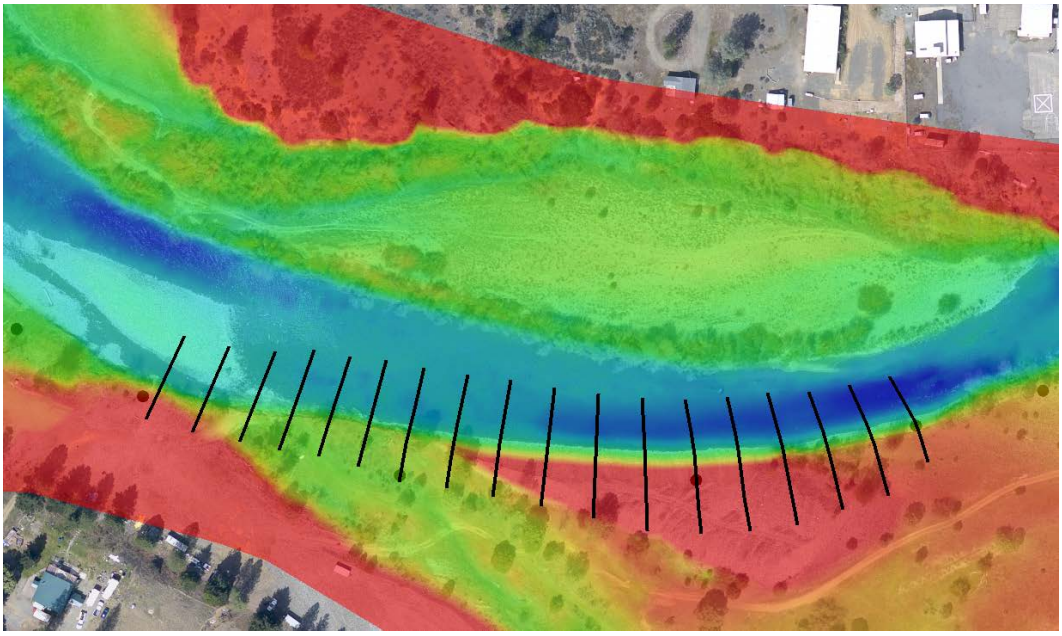

Figure 22. Sixteen bank cross sections (black lines) used for a coupled modeling between SRH-2D and bank erosion model.

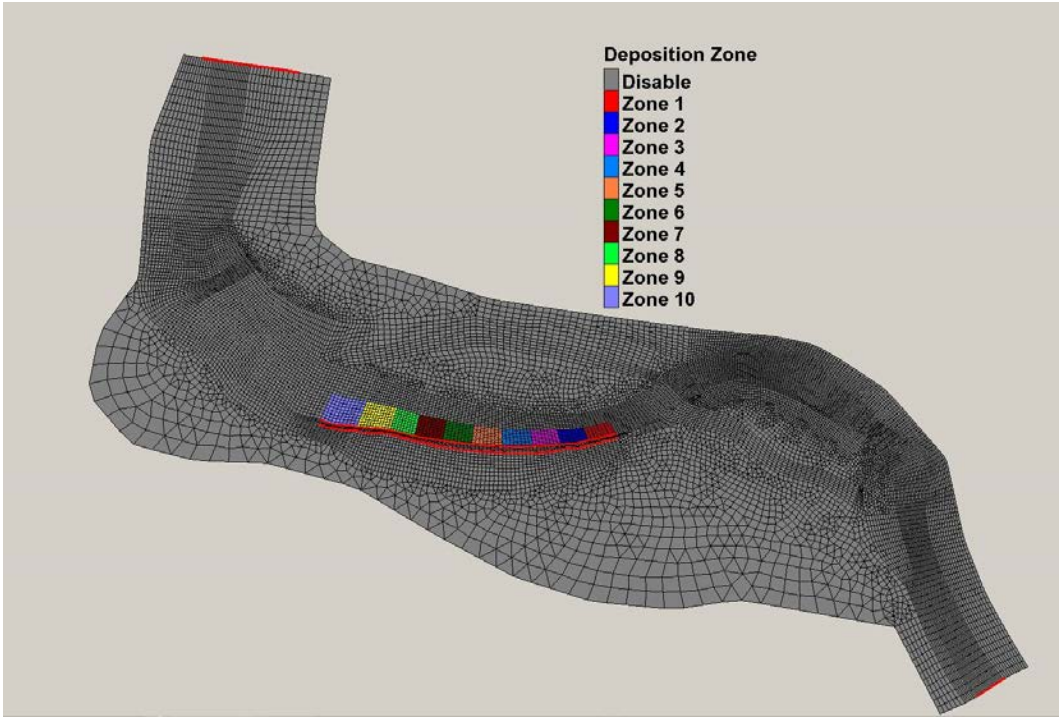

Figure 23. Deposition zones used to add the eroded bank materials to the stream.

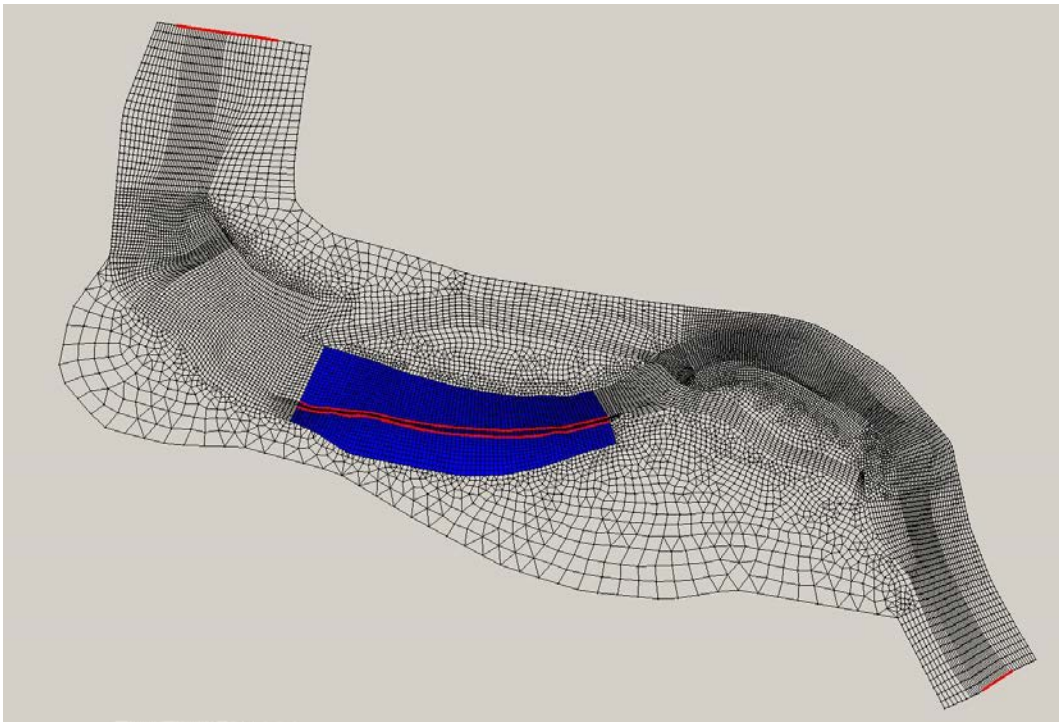

Figure 24. The mesh zone (the blue area) used in which mesh points were moved and deformed when banks were retreating.

4 Results of Preliminary Modeling Condition

Preliminary modeling was carried out first as discussed in the Introduction. SRH-2D was modified to accept the BSTEM-predicted bank-generated sediment loadings as lateral inputs to the stream. Model runs - named "preliminary modeling" (PM) - were then carried out. The PM cases were not calibrated due to limited time available; they were intended for obtaining quick turn-around results for project impact assessment. Coupled morpho-dynamic and bank erosion modeling was time consuming and would not produce results until the project was completed. Therefore, the results produced by PM runs discussed below should be viewed as tentative; results of the coupled morpho-dynamic and bank erosion modeling in Chapters 5 and 6 are expected to be more accurate.

Both "design construction" scenario (DC) and 2011 "post-erosion condition" (PC) scenario were simulated. Each scenario had two modeling runs: without and with bank-generated sediment materials added to the stream. A total of four runs were carried out; they were named PM-DC-NL (design construction without lateral sediment loadings), PM-DC-WL (design construction with sediment loadings), PM-PC-NL (post-erosion condition without sediment loadings), and PM-PC-WL (post-erosion condition with sediment loadings). For the PM-DC-WL and PM-PC-WL runs, BSTEM-predicted lateral sediment loadings in Cardno ENTRIX (2012), discussed in Section 2.2, were added to the stream.

The predicted net erosion and deposition of the four runs are compared in Figure 25 and Figure 26. The differences of the predicted net erosion and deposition depth between PM-DC-WL and PM-DC-NL and between PM-PC-WL and PM-PC-NL are shown in Figure 27. The model results showed that adding bank sediments to stream had small effects on the upstream half of the study reach under the DC (design construction) scenario; however, it had noticeable effects in the upstream half of the reach under the PC (2011 post-erosion condition) scenario. The impact on the downstream half of the reach was significant if the BSTEM predicted bank sediments were added to the stream; it led to an increased deposition downstream under both the DC and PC conditions.

The model results are plotted in another way in Figure 28 for project impact assessment. The differences of the predicted net erosion and deposition depth between the DC and PC scenarios are shown. Positive depth value indicates that the bed elevation under the DC scenario is lower than that of the PC scenario and vice versa. Figure 28 provided information about the morphological impact incurred by the design construction. For ease of discussion, terminologies used to designate different features of the design construction are shown in Figure 29. These terminologies are used for the remaining part of the report when model

results are discussed. The PM modeling results pointed to the following potential issues with the design construction scenario:

- The left and right side channels were predicted to have the potential to be filled with sediments. It is possible that the neglect of lower flows (<4,000 cfs) exacerbated the predicted deposition in the side channels.
- Deposition in the left split channel was also predicted.
- The bank erosion zone, where the bank experienced significant erosion between 2009 and 2011, was predicted to have a higher rate of bank erosion caused by the design construction than the 2011 post-erosion scenario when eroded bank sediments were not added to the stream. However, the trend reversed if the BSTEM predicted bank sediments were added to stream.

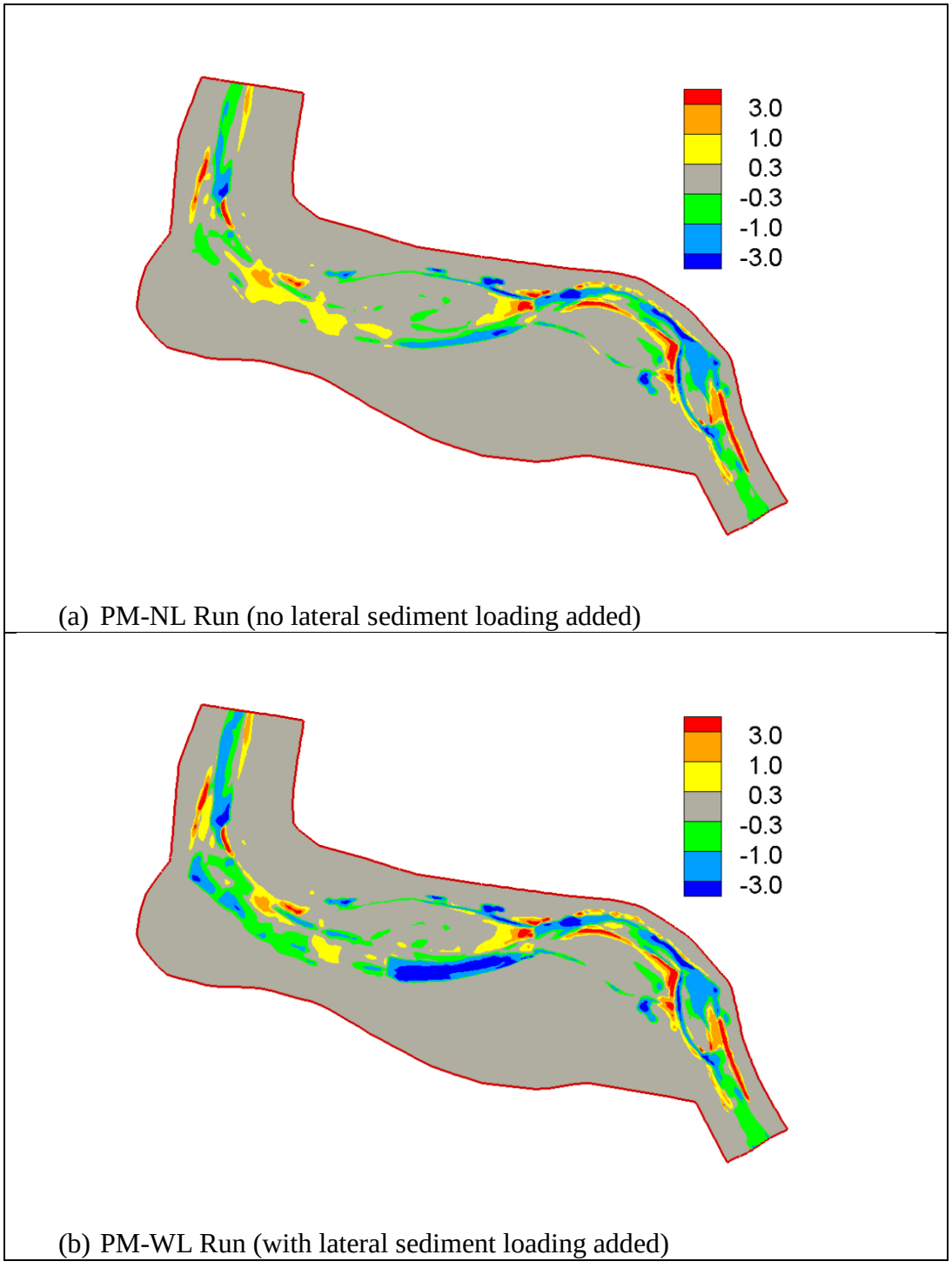

Figure 25. Predicted net erosion (positive) and deposition (negative) depth in feet for the PM-NL and PM-WL runs under the design construction condition.

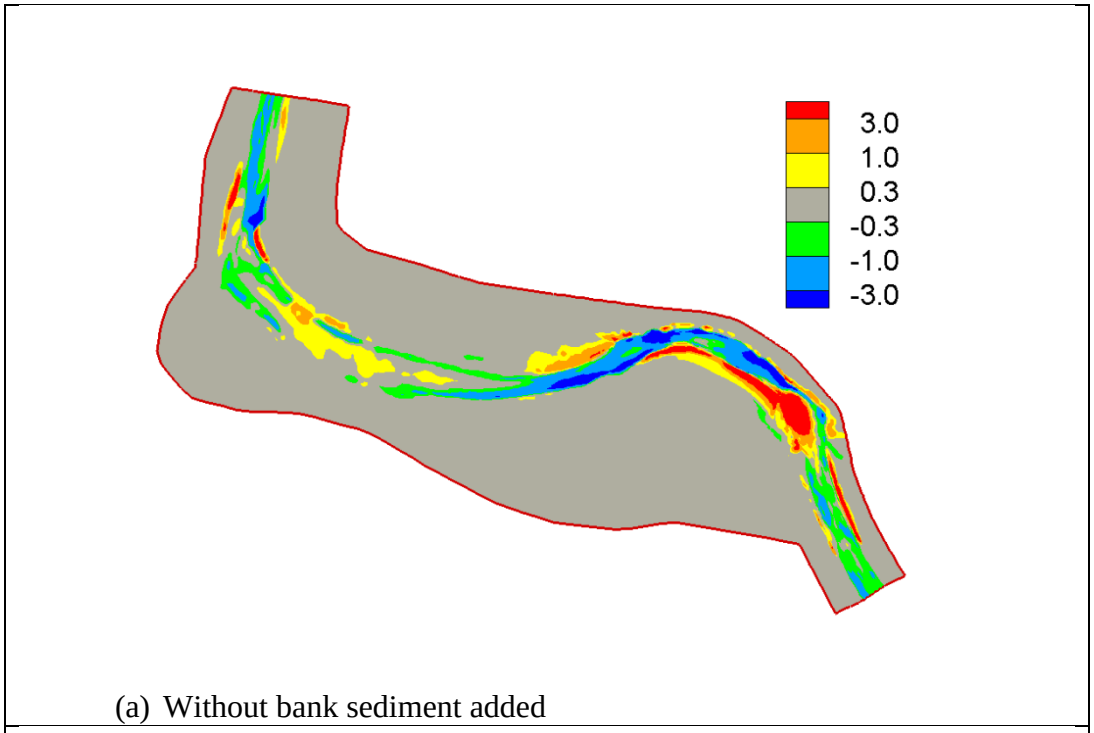

(a) Without bank sediment added

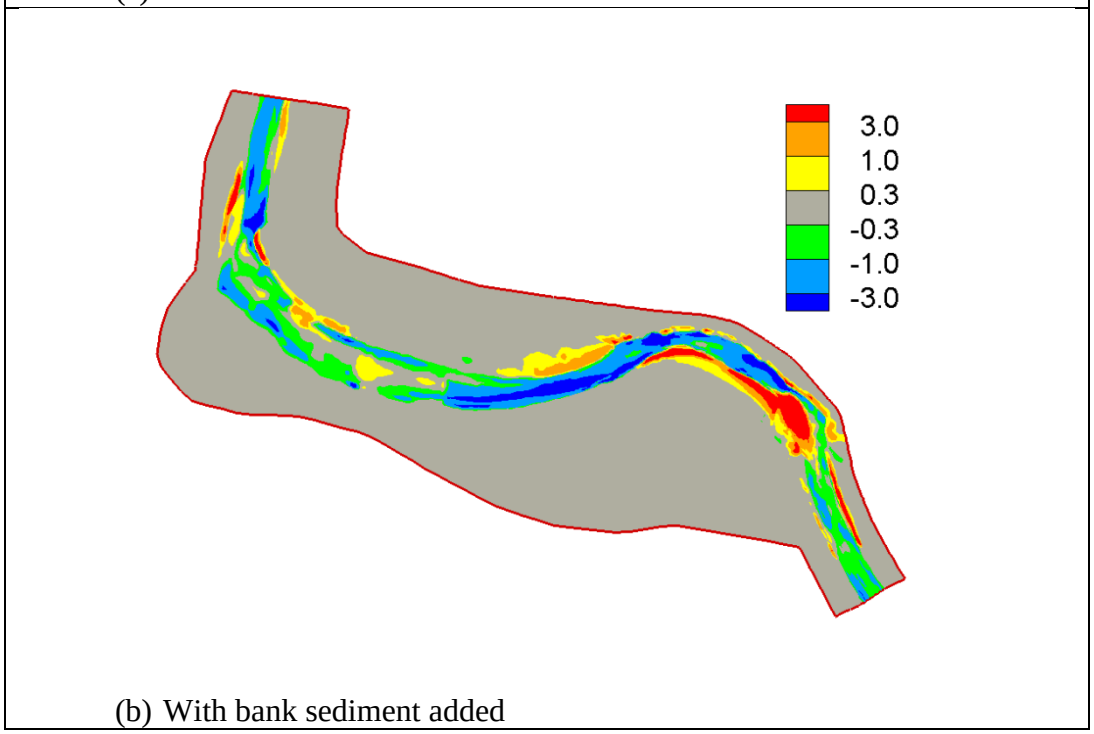

(b) With bank sediment added

Figure 26. Predicted net erosion (positive) and deposition (negative) depth in feet for the PM-NL and PM-WL runs under the 2011 post-erosion condition.

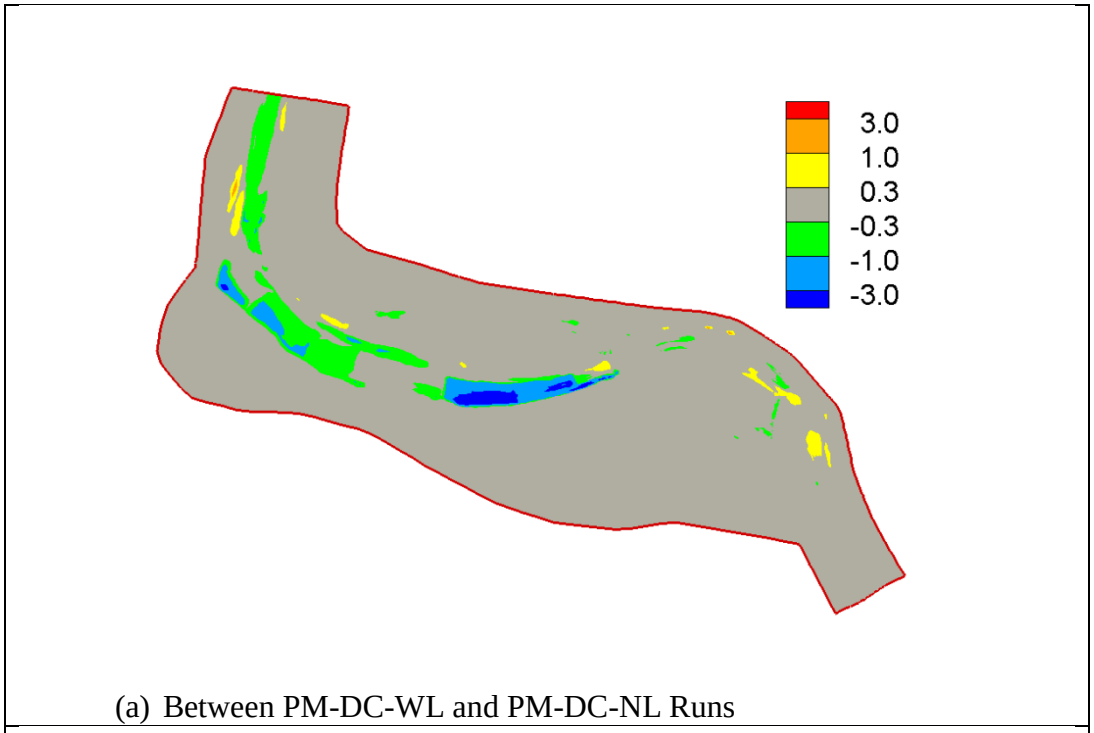

(a) Between PM-DC-WL and PM-DC-NL Runs

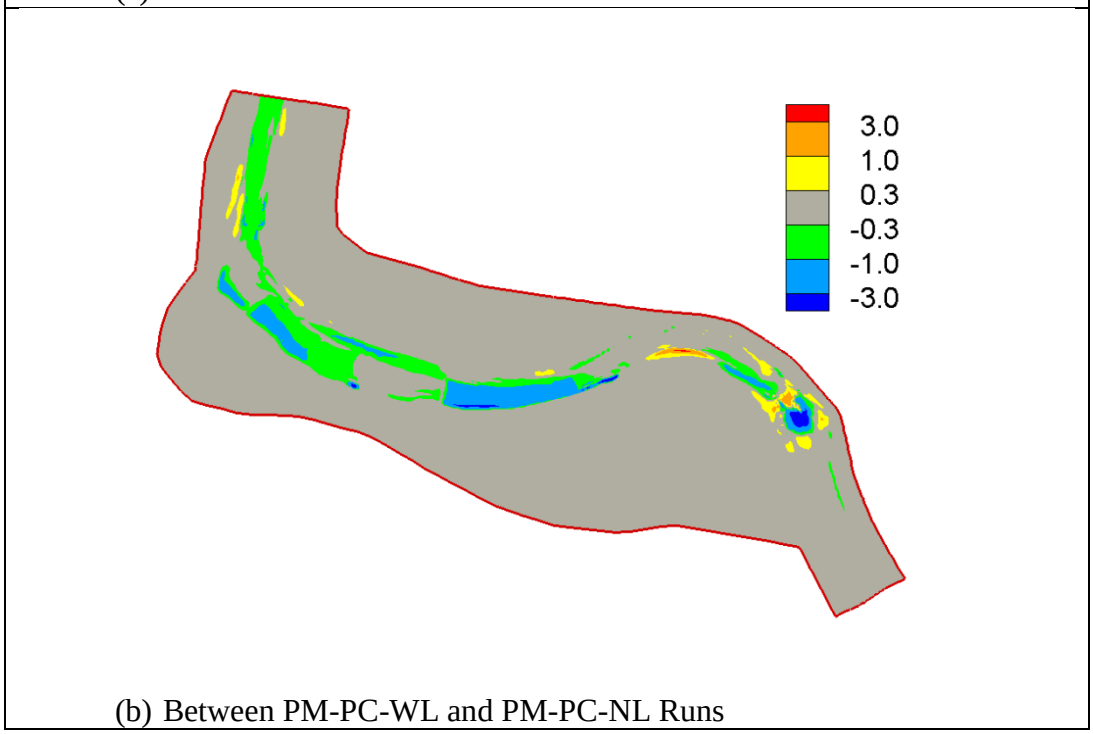

(b) Between PM-PC-WL and PM-PC-NL Runs

Figure 27. Differences of the predicted erosion depth in feet; positive if the WL (with loading) run predicted a lower bed elevation than the NL (without loading) run.

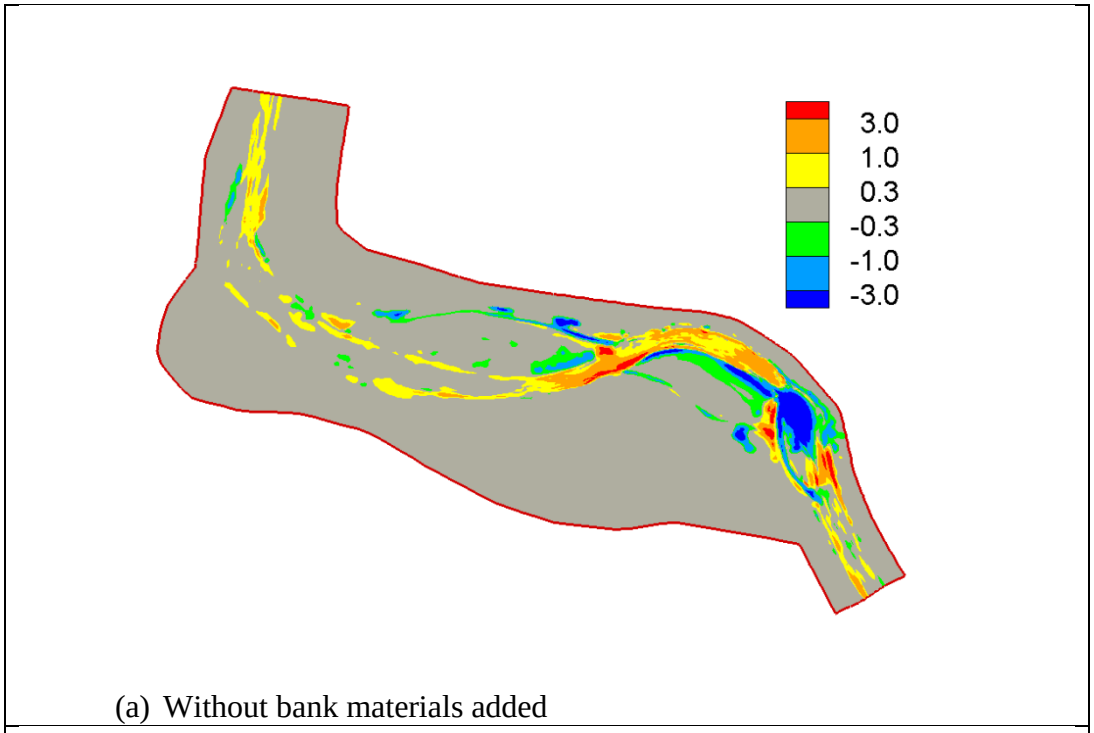

(a) Without bank materials added

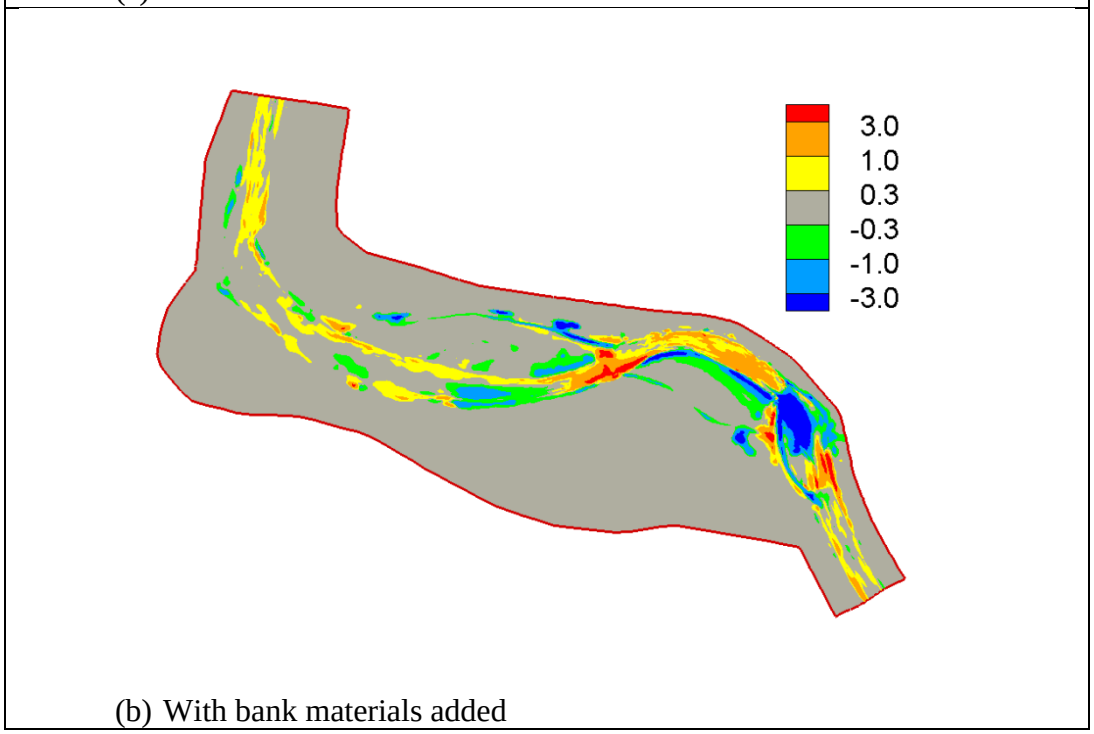

(b) With bank materials added

Figure 28. Differences of the predicted net erosion and deposition depth in feet between the DC (project design) condition and the PC (post-erosion) condition; positive if the DC run predicted a lower bed elevation than the PC run.

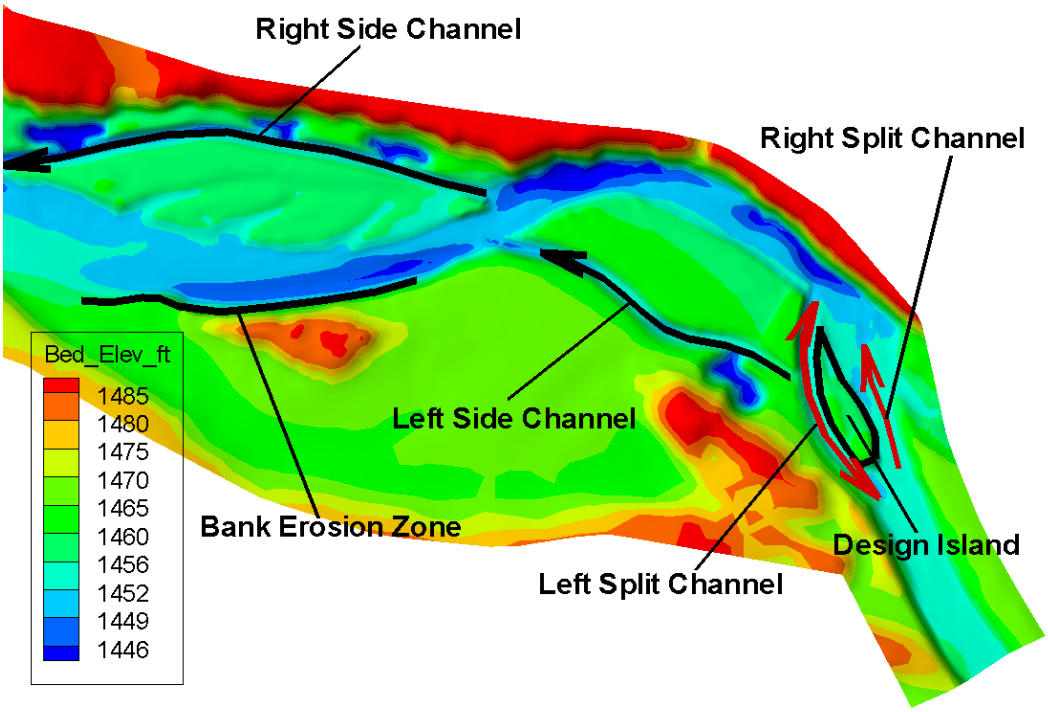

Figure 29. Schematic showing the terminology used to identify different features of the design construction.

5 Results of 2009 Pre-Project Baseline Condition

A series of runs were made under the 2009 pre-erosion baseline (PB) condition for the purpose of calibration of the coupled model. They also served as verification studies to understand what the current state-of-the-art 2D models, such as SRH-2D with coupled morpho-dynamic and bank erosion modeling, could achieve in modeling gravel bed streams with riffles and pools. Note that no separate flow modeling calibration was carried out.

5.1 Baseline Model Results

A baseline model run was developed so that other model runs under the PB condition could be compared to it. The baseline model was calibrated with a number of input parameters and it had the following model inputs in addition to what has been discussed in Chapter 3:

(1) The sediment transport capacity equation was based on the Trinity equation presented in equations (2) to (4); and
(2) The adaptation length was based on that derived from the study of Seminara et al. (2002) as documented by Lai (2013) (also discussed in the next section).

The baseline model results are presented in this section while sensitivity results are discussed in the next.

The net erosion and deposition depth between the 2009 and 2011 terrains is shown in Figure 30. The survey data suggested that the three pools, marked as "Pool 1," "Pool 2" and "Pool 3," were subject to deposition while a section of the left bank, marked as "Bank Erosion," experienced significant bank erosion. We would like to investigate what a 2D geofluvial model such as SRH-2D could accomplish in modeling gravel rivers such as the Trinity River. It has been known (e.g., Logan et al. 2010) that the sediment transport and morphologic modeling of riffle-pool systems is challenging with any numerical models. Few existing morphological models are available to simulate lateral bank erosions.

Two baseline model runs were carried out: one without the use of the bank erosion model (named PB-No-Bank) and another with the bank erosion model (named PB-With-Bank). The predicted net erosion and deposition are compared with the measured data in Figure 31 and Figure 32; zoomed-in views of the same plots are displayed in Figure 33. In addition, the predicted bed elevation changes in time at the deepest points of Pool 1 and Pool 2 are plotted in Figure 34.

The model results showed that bank erosion on the left was not predicted with the PB-No-Bank run; it pointed to the need to use the bank erosion model. The PB-With-Bank run was capable of predicting bank erosion on the stream left by simply using the measured and BSTEM estimated bank parameters. No attempt was made in this study to improve the model prediction of bank retreat rates by changing the critical shear stress or erodibility.

A comparison of PB-No-Bank and PB-With-Bank results showed that the eroded bank sediments were mostly deposited in the stream near the eroded bank and were not transported to downstream very far, at least during the simulation period. More than 50% of the eroded bank sediments were large gravels and small cobbles at banks UJC-E and UJC-F; they were less movable once deposited in the stream. As a result, the impact of the eroded bank sediments on the downstream half of the reach was relatively small.

Upstream of the bank erosion zone, both PB-No-Bank and PB-With-Bank runs were capable of predicting qualitative erosion and deposition patterns. The differences in results of the two runs were relatively small in the upstream half of the reach. Therefore, the PB-No-Bank run could be used to assess the model capability to predict the riffle-pool processes at this site.

Two main discrepancies were identified between model predictions and measured data. First, the model predicted much more deposition than the measured data in the three pools. Second, the riffle erosion downstream of Pool 2 was not predicted by the model. The predicted bed elevation changes at the deepest points of the first two pools are plotted in Figure 34. A total of 5 and 8 feet of deposition were predicted in Pool 1 and 2, respectively; the corresponding measured depositions were approximately 2.2 and 3.2 feet. This over-prediction of the pool filling process has been a consistent problem with any depth-averaged numerical models since such models do not take the horizontal vortices into consideration. 3D models may have the potential to improve the predictions; but this is yet to be proven. Other factors might contribute to the over-prediction of the pool filling process. High uncertainty in the initial bed gradation specification of the riffle areas was one of them. Over-prediction of erosion at riffles might lead to increased deposition in the downstream pool. Sediment transport capacity equations may also may be the cause of the poor predictions as most existing ones are based on reach-averaged or depth-averaged variables.

Riffle erosion downstream of Pool 2 was predicted after first 2009 and 2010 runoffs as shown in Figure 31a and Figure 32a; however, the area was depositional after the 2011 runoff. The reason for the failure of the numerical model to predict the riffle erosion in the area was unclear. It might be caused by factors such as inaccuracy in initial bathymetry and/or bed gradation, neglect of bank vegetation impact, or too much upstream sediment supply at high discharges. The most probable cause was conjectured to be the existing mature

vegetation along the nearby right bank which was under water only at high discharges in 2011 but not represented by the model.

Downstream of the bank erosion zone, model results were less accurate since the downstream stage-discharge rating curved used might have high uncertainty. There was not enough measured net erosion and deposition data near the downstream boundary so it was difficult to assess.

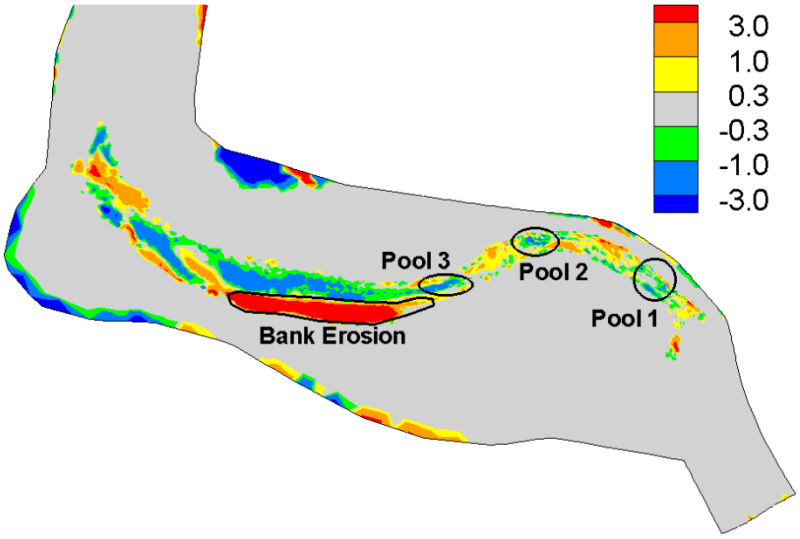

Figure 30. Measured net erosion (positive) and deposition (negative) depth in feet between the 2009 and 2011 terrains.

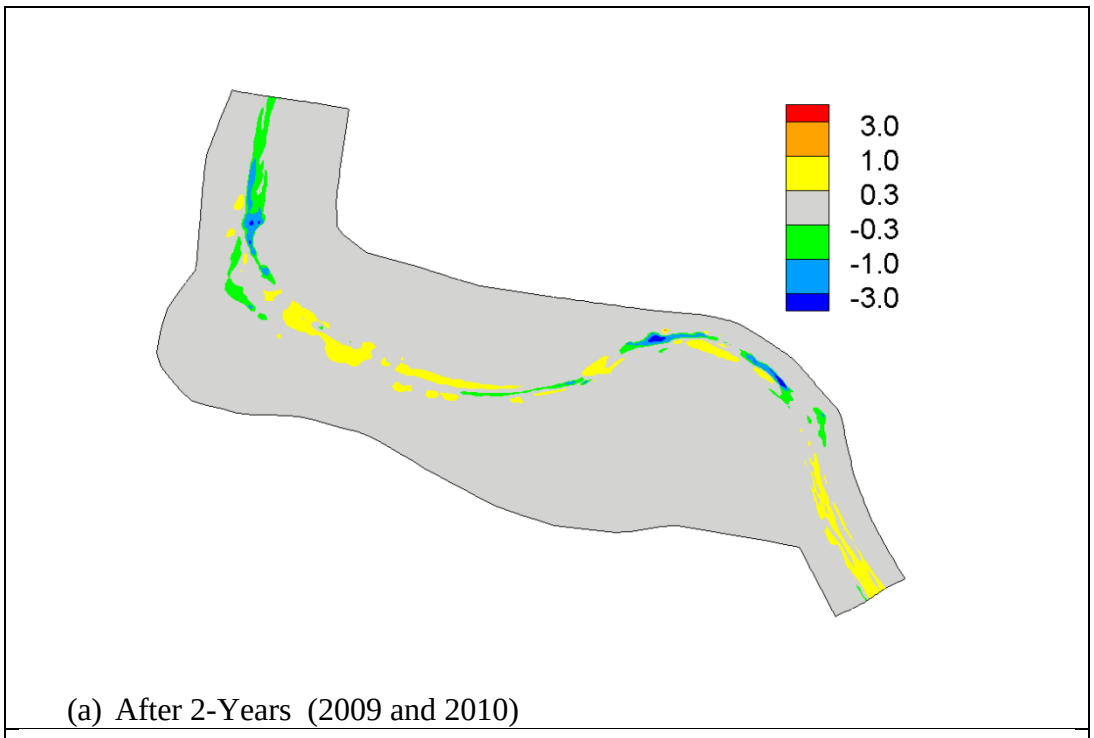

(a) After 2-Years (2009 and 2010)

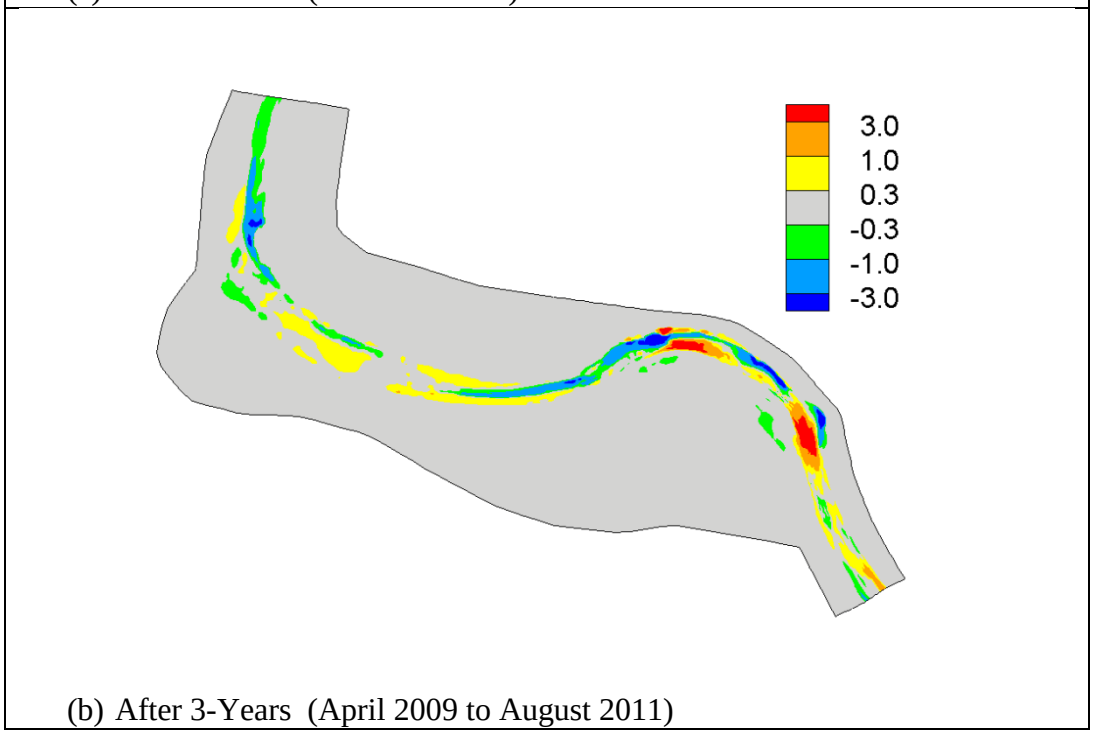

(b) After 3-Years (April 2009 to August 2011)

Figure 31. Predicted net erosion (positive) and deposition (negative) depth in feet with the PB-No-Bank run.

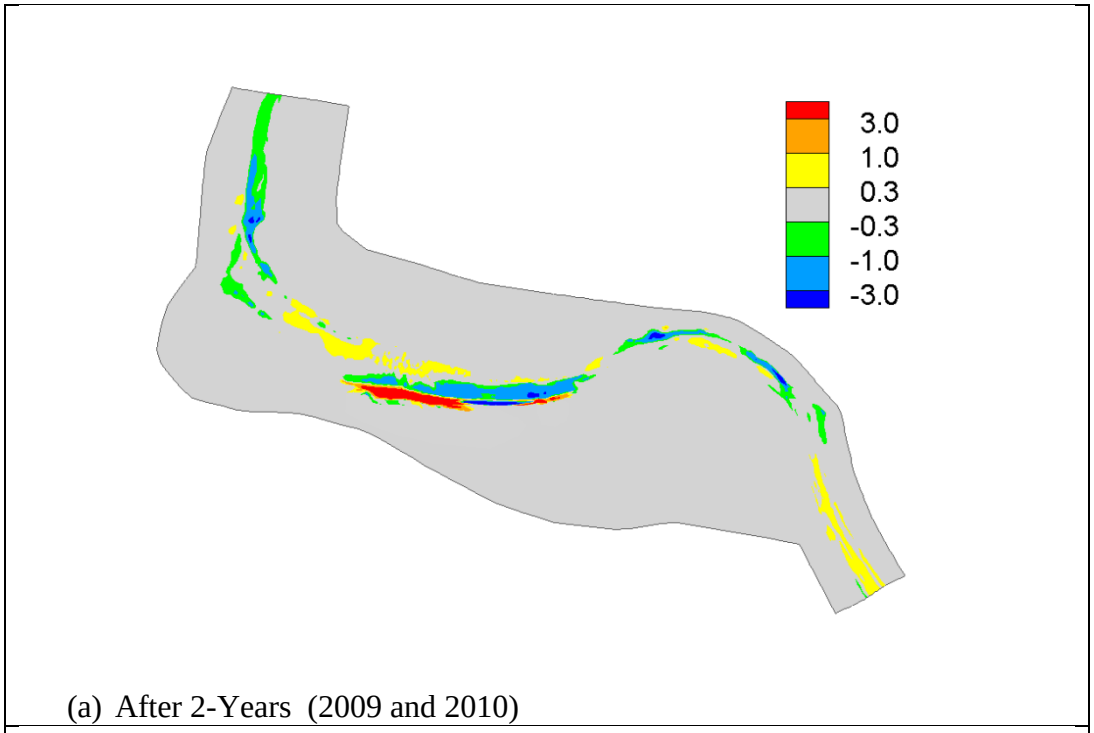

(a) After 2-Years (2009 and 2010)

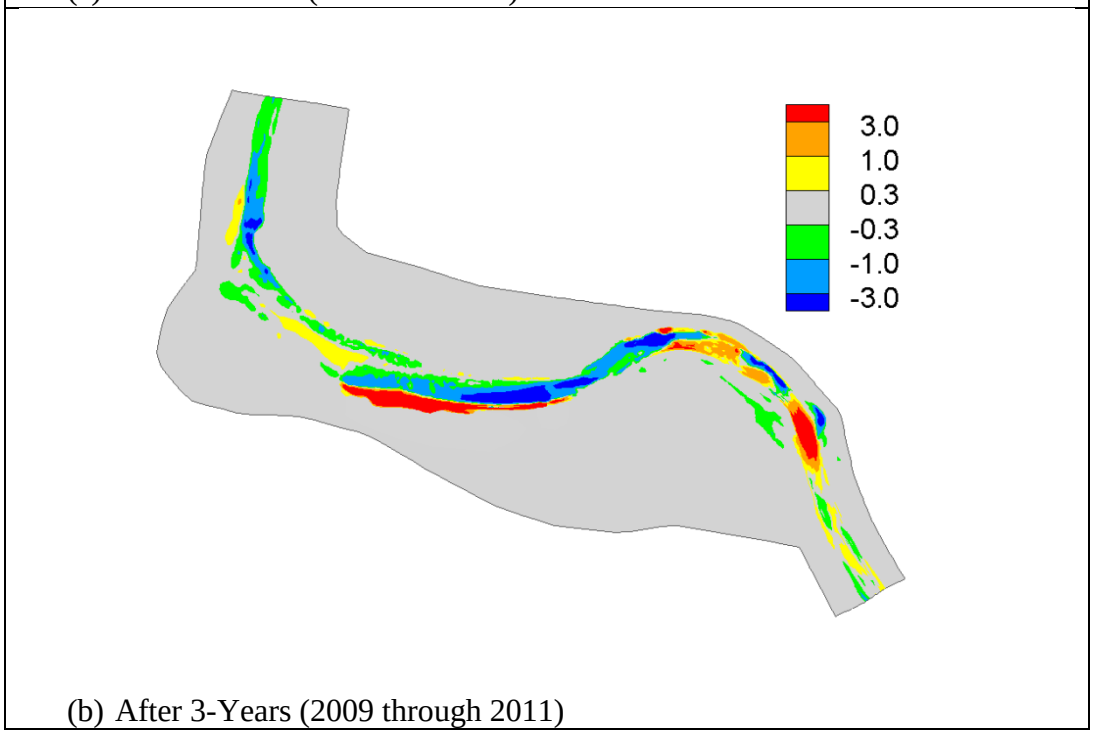

(b) After 3-Years (2009 through 2011)

Figure 32. Predicted net erosion (positive) and deposition (negative) depth in feet with the PB-With-Bank run.

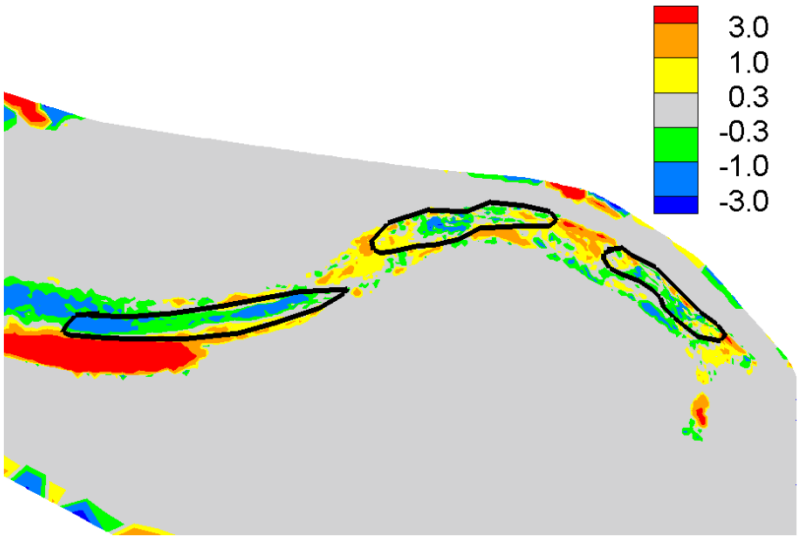

(a) Measured Data

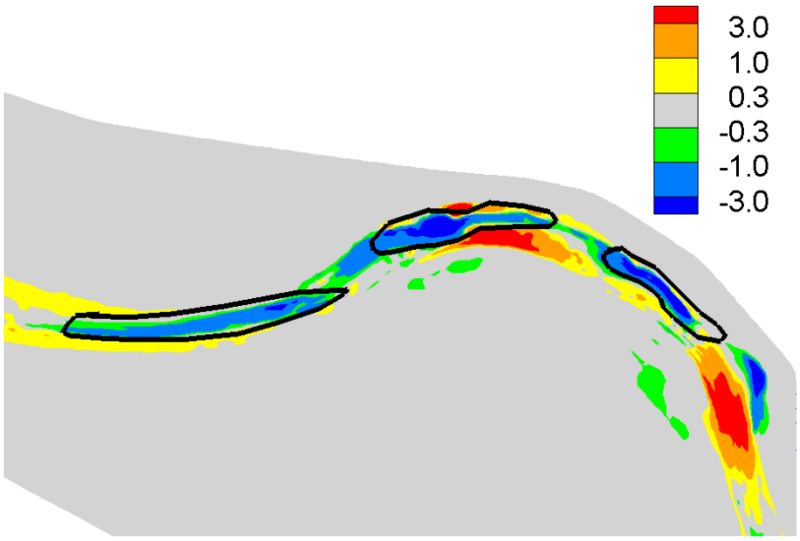

(b) Prediction with PB-No-Bank Run

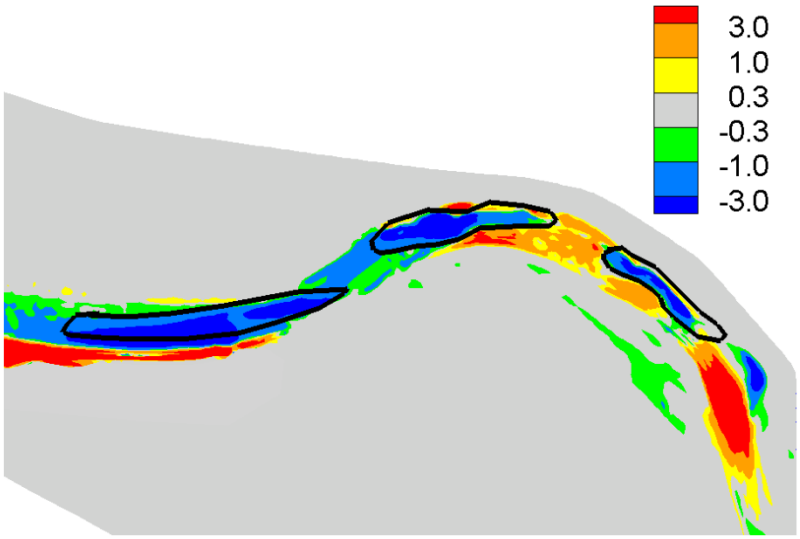

(c) Prediction with PB-With-Bank Run

Figure 33. Zoom-in views of the predicted and measured pool-filling after 3-year runoffs (2009 through 2011).

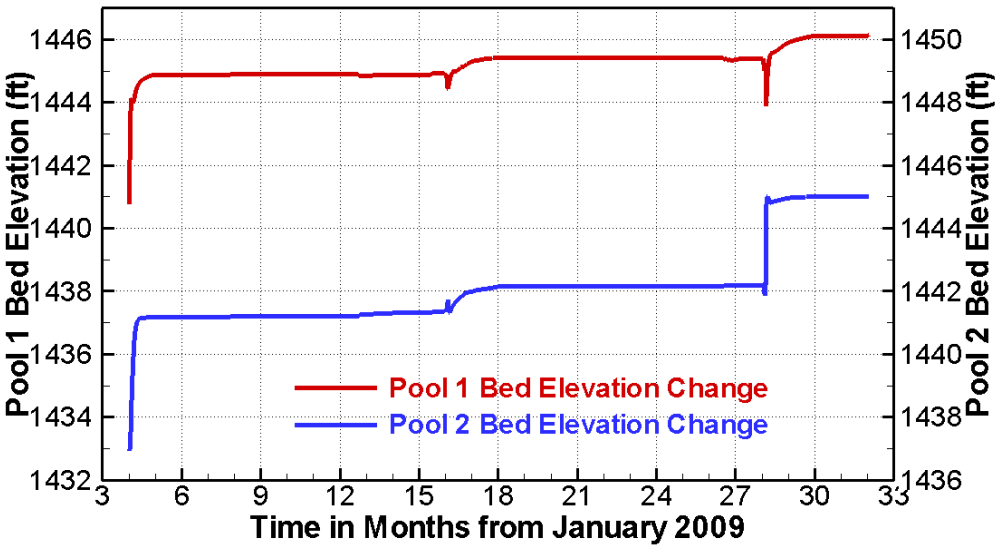

(a) Prediction with PB-No-Bank Run

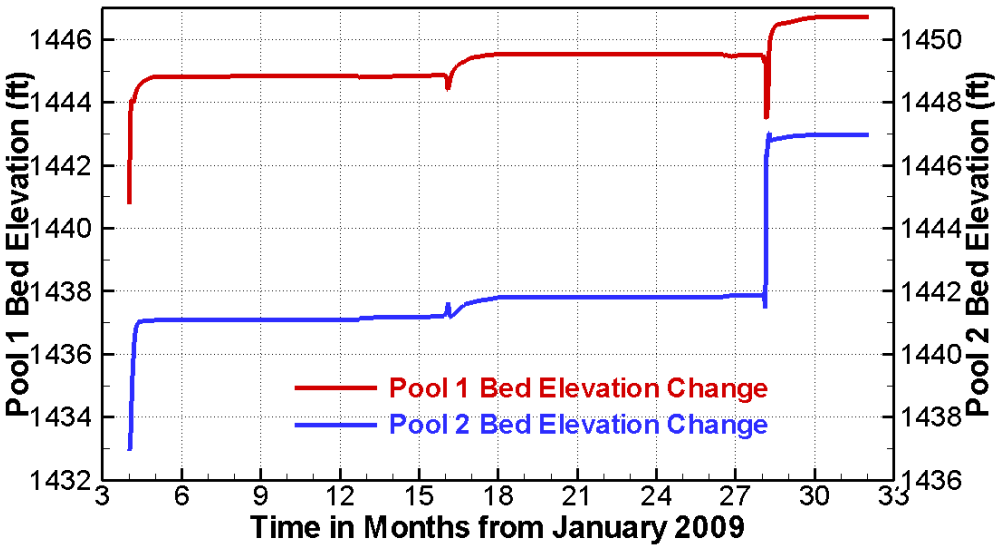

(b) Prediction with PB-With-Bank Run

Figure 34. Predicted bed elevation variations in time at the deepest points of Pool 1 and Pool 2.

5.2 Sensitivity Studies

Sensitivity studies were carried out under the PB condition using the No-Bank model since the difference between the No-Bank and With-Bank runs was relatively small in predicting the riffle-pool processes upstream of the bank erosion zone.

Sediment transport capacity equations and bedload adaptation length are two of the most important input parameters for morphological modeling in streams. The capacity equation provides erosion potential with non-equilibrium models; it is not the actual sediment transport rate in streams. Many capacities equations have been developed based on mostly reached averaged data and no single equation has worked well for all streams. The adaptation length quantifies the travel distance required for a packet of sediment to reach a new equilibrium concentration when it moves into a region of higher or lower shear stress. Widely different suggestions have been made with regard to its value and no consensus has been reached. In this study, a number of sensitivity studies were carried out with regard to the above two inputs.

A number of transport capacity equations, suitable for gravel rivers, have been implemented in SRH-2D. In addition to the Trinity equation (Gaeuman et al., 2009) and the Wilcock-Crowe equation presented in equations (2) to (5), another capacity equation developed by Seminara et al. (2002) was added into SRH-2D and tested. The rates at which bedload particles of a grain size *k* are entrained (E_k) and deposited (D_k) are given as (Seminara et al., 2002):

$$\frac{E_k}{\sqrt{(s-1)gd_k}} = \alpha\left(\theta_k - \theta_{k,c}\right)^{3/2} \tag{6a}$$

$$\frac{D_k}{\sqrt{(s-1)gd_k}} = \beta\left(\theta_k - \theta_{k,c}\right)^{1/2} \xi_k^* \tag{6b}$$

Here, *s* is the specific weight of the sediment, *g* is gravitational acceleration, α and β are numerical constants equal to 0.0199 and 0.03, respectively, $\theta_k = \tau_b / \left[\rho g(s-1)d_k\right]$ is the Shield's parameter of sediment size class *k*, and ξ_k^* is a dimensionless bedload concentration, given by:

$$\xi_k^* = \frac{hC_k}{d_k} \tag{7}$$

The above entrainment and deposition rates were directly implemented into SRH-2D. This approach essentially produced a new sediment transport capacity equation solved numerically.

The Seminara et al. (2002) equations were also used to derive a new adaptation length expression in this study. The entrainment and deposition rates in (6) and (7) were transformed into the following form:

$$S_{e,k} = E_k - D_k = \frac{1}{L_{b,k}}\left(q^*_{b,k} - q_{b,k}\right) \tag{8a}$$

$$q^*_{b,k} = \frac{\alpha}{\beta} V_s d_k \left(\theta_k - \theta_{k,c}\right) \tag{8b}$$

$$q_{b,k} = V_s h C_k \tag{8c}$$

$$L_{b,k} = \frac{V_s d_k}{\beta\sqrt{(s-1)g d_k}\sqrt{\theta_k - \theta_{k,c}}} = \frac{V_s d_k}{\beta\sqrt{(\tau_b - \tau_{cri})/\rho}} \tag{8d}$$

In the above, $V_s = \beta_k V_t$ is the sediment movement velocity, $q^*_{b,k}$ is the transport capacity rate, and $L_{b,k}$ is the bedload adaptation length. Equation (8d) is a new bedload adaptation length that was implemented in SRH-2D and was used together with the Trinity capacity equation.

In addition, Seminara et al. (2002) study determined that the bed load saltation length could be computed as:

$$L_{b,k} = 286.4 d_k \tag{9}$$

Equation (9) itself was used as the third option to compute the bedload adaptation length.

Three runs were carried out with regard to the sensitivity of model results to the bedload adaptation length. They were named PB-No-Bank, PB-No-Bank-A2 and PB-No-Bank-A3. All three runs used the Trinity capacity equation but with different adaptation length equations. PB-No-Bank was the baseline model run that used the constant length of 80 meters that was about 2.5 times the average channel width; PB-No-Bank-B2 adopted the Seminara equation in (8d); PB-No-Bank-A3 utilized equation (9). The model results of the three runs are shown in Figure 35. The results showed that the difference between PB-No-Bank and PB-No-Bank-A2 was insignificant; however, the use of equation (9) with the PB-No-Bank-A3 run led to large difference, particularly in the reach upstream of the pools. More deposition was predicted with the PB-No-Bank-A3 run.

Three additional cases were compared with regard to the use of different transport capacity equations. They were named PB-No-Bank, PB-No-Bank-C2, and PB-No-Bank-C3. PB-No-Bank was the baseline model run that uses the Trinity capacity equation; PB-No-Bank-C2 used the Seminara et al. (2002) equations in (6); and PB-No-Bank-C3 used the Wilcock-Crowe (2003) equation. The results with the Seminara et al. (2002) equations were found to be unrealistic since they predicted significantly higher erosion over the entire channel than the survey data.

Therefore, the PB-No-Bank-C2 results presented below were based on the run with a much smaller α coefficient of 0.00199 (the original equation used 0.0199). The results of the three runs are shown in Figure 36. It is seen that the Seminara et al. capacity equation predicted similar net erosion and deposition results as the Trinity capacity equation, but only after a factor of 10 reduction in the computed capacity. Therefore, the Seminar et al. capacity equation might not be adequate in predicting the bedload transport for the Trinity River. The Wilcock-Crowe capacity equation produced too much erosion in the channel and the results did not seem to be reasonable. It is noted that the use of higher sediment capacity rate increased the erosion but the pool-filling was still over-predicted. It suggested that the prediction of the pool-filling processes would not be improved if the same capacity equation was applied over both deposition and erosion zones. Different pickup rate (capacity) equations or adaptation length equations might be needed in erosion and deposition zones to improve the pool-filling prediction.

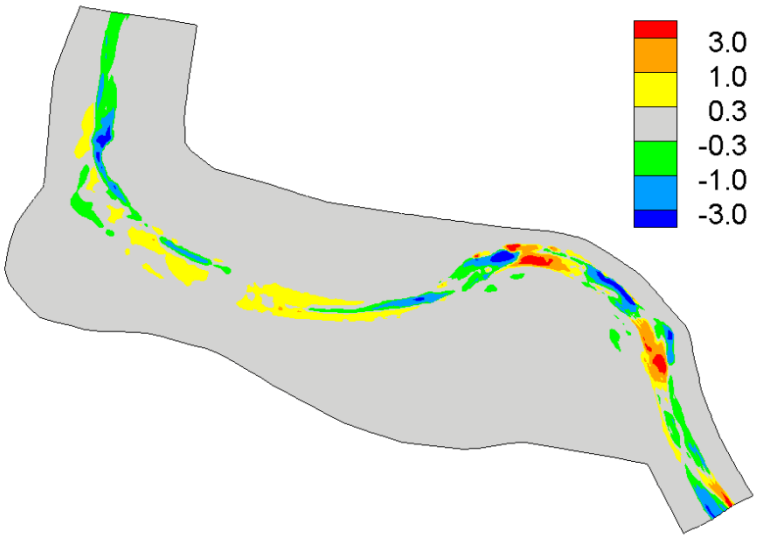

(a) PB-No-Bank

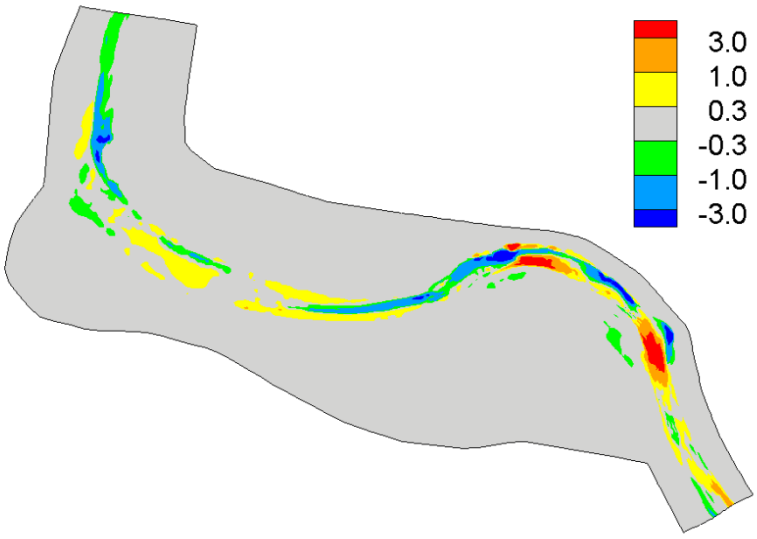

(b) PB-No-Bank-A2

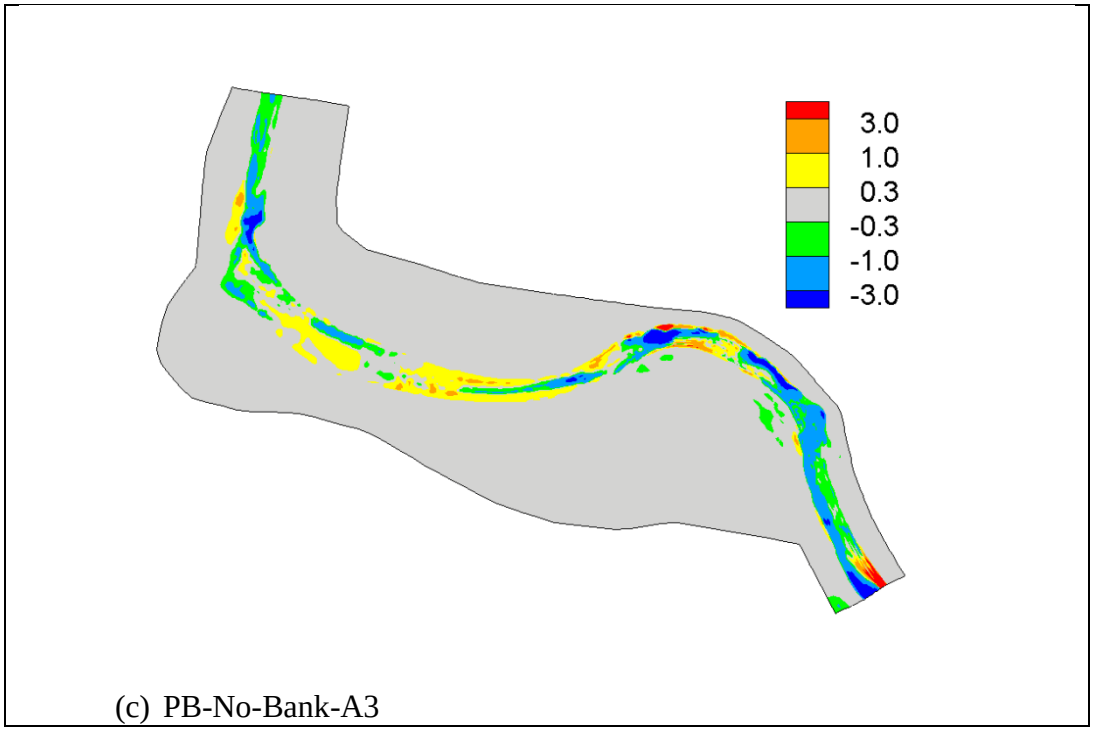

(c) PB-No-Bank-A3

Figure 35. Sensitivity of the predicted net erosion (positive) and deposition (negative) depth in feet to the adaptation length equations.

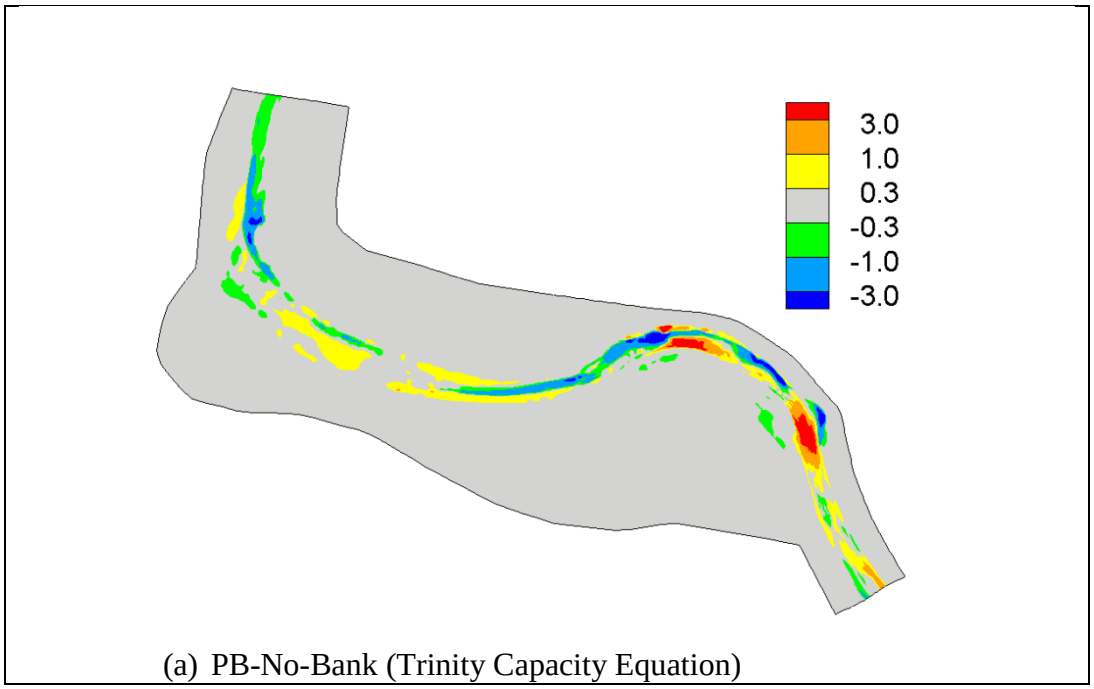

(a) PB-No-Bank (Trinity Capacity Equation)

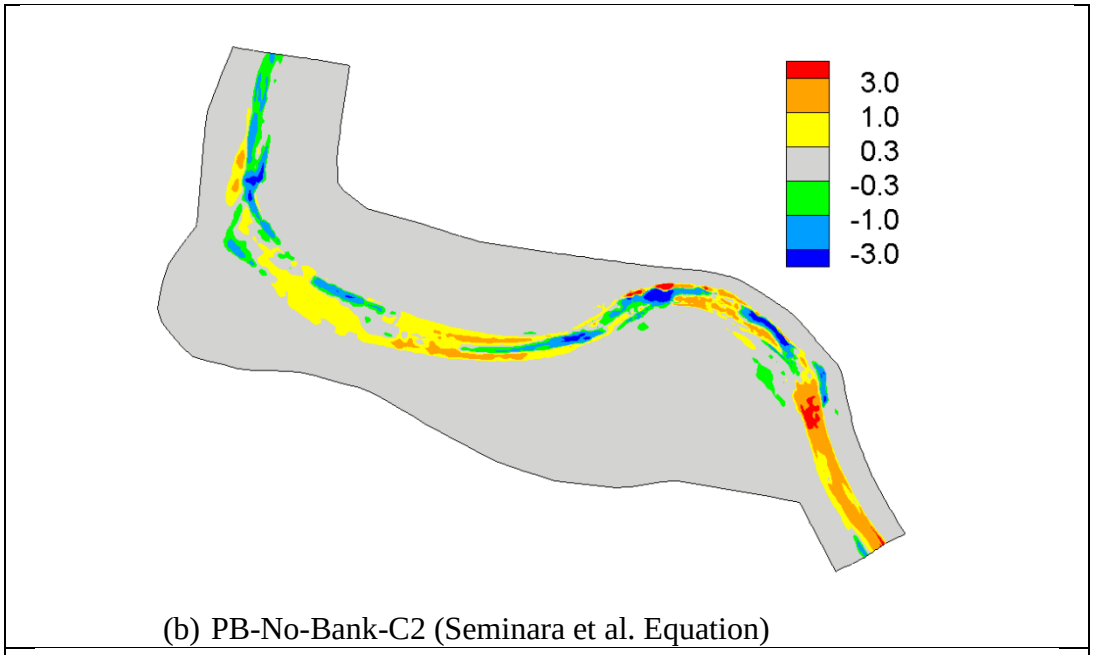

(b) PB-No-Bank-C2 (Seminara et al. Equation)

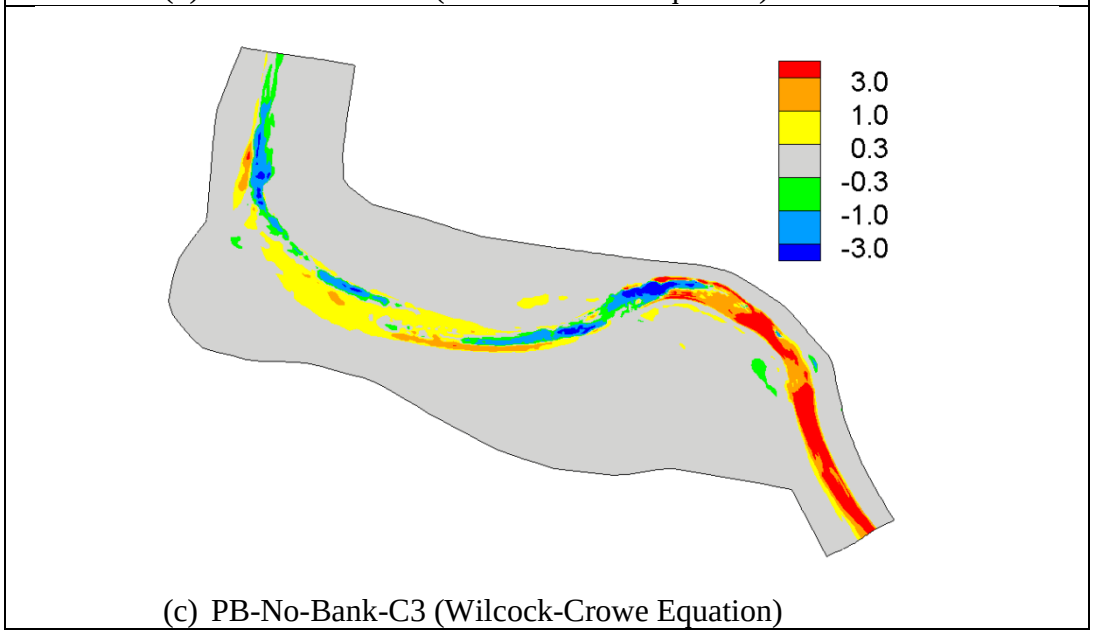

(c) PB-No-Bank-C3 (Wilcock-Crowe Equation)

Figure 36. Sensitivity of the predicted net erosion (positive) and deposition (negative) depth in feet to the sediment transport capacity equation.

6 Results of Morphologic Assessment Condition

6.1 Description of Project Impact Assessment Runs

The calibrated and verified model was next applied to assess the impact of the rehabilitation project on stream morphology at the UJC site. It is expected that the pool-filling processes would not be predicted well but processes such as the bank erosion, side channel filling with coarser sediments, and vertical stream bed change downstream of the three pools would be predicted. The model runs in this chapter were named the "morphologic assessment" (MA) runs. Two scenarios were created under the MA condition: PC (2011 post-erosion condition) and DC (2012 design construction) scenarios. The design construction was simulated, not the actual constructed project. The project construction started in June 2012 and completed in November 2012. The actual construction data was unavailable at the start of this study. The two scenarios used the same models except for the initial terrain. Therefore, the differences between the two were due to the project design only.

For the MA runs, the flow hydrograph from April 2009 to September 2011 was used. The cut-off discharge, however, was 4,000 cfs to reduce the computing time to a reasonable level. The use of a higher cut-off discharge would not change the project impact assessment conclusions since significant stream morphology changes would mainly be caused by high-discharge flows. It is cautioned, however, the suspended sediment deposition in the side channels and on the floodplain might be under-predicted due to the use of the cutoff discharge.

Two runs were carried out using the coupled morpho-dynamic and bank erosion model: MA-PC and MA-DC. MA-PC is the run with the 2011 post-erosion condition scenario while MA-DC run is the 2012 design construction scenario. The predicted net erosion and deposition of the two runs are shown in Figure 37 and zoom-in views of the results are in Figure 38. The differences of the predicted net erosion and deposition between the MA-DC and MA-PC were digitally processed and are plotted in Figure 39. Positive depth in Figure 39 means that the bed elevation of the MA-DC scenario was lower than that of the MA-PC scenario and vice versa.

6.2 Modeling Summaries

The following conclusions may be drawn based on the model results under the MA condition (for location terminology, see Figure 29):

- Deposition was predicted in both the left and right side channels as seen in Figure 37a. The model results after 2009 and 2010 runoffs are further plotted in Figure 40. A comparison of the predicted deposition in the two side channels between Figure 40 and Figure 37 showed that the predicted deposition occurred mainly during the 2011 runoff. The peak discharge is 6,040 cfs and 7,520 cfs, respectively, in 2009 and 2010; while the peak is 12,900 cfs in 2011. Therefore, the predicted side channel deposition was mainly due to flows higher than 12,000 cfs.
- The only side channel deposition that might be of concern for the project was the entrance zone of the downstream right side channel. Increased deposition risk was expected with increased flows higher than 12,000 cfs.
- The predicted side channel deposition may not be a concern for other locations of the two side channels. For the upstream left side channel, the entrance to the side channel was predicted to have erosion (Figure 38) if the initial bed materials in the entrance were the same as the main channel (d_{50}=29 mm). This entrance erosion may not be a problem since the actual construction used much coarser sediments. Slight deposition was predicted downstream of the entrance zone in the left side channel (including the pool). However, only fine sediments, less than 10 mm, were deposited based on the predicted medium sediment size distribution in Figure 41 and Figure 42. For the downstream right side channel, deposition is limited to the entrance and three side channel pools. Again, only fine sediments were predicted to deposit and they were not considered to be a concern.
- A major potential impact of the design construction, based on the model results, is that the main channel downstream of the design island might experience less deposition in some areas and more erosion in others (see Figure 39). However, the left bank zone was not predicted to experience higher rate of lateral erosion than the 2011 post-erosion condition due to the design construction (compare results in Figure 37). On the contrary, the design construction was predicted to lead to slightly less bank erosion. Less deposition in the stream near the bank erosion zone was probably due to less bank erosion predicted with the design construction scenario. Note that the modeling did not consider other bank sections.
- The model predicted some deposition in the left split channel of the design island and erosion on the right split channel. In view that the 2011 post-erosion scenario was predicted to be erosional in the same area, the right spilt channel erosion may not be a concern. The left split channel deposition might be an important risk to consider since the deposited sediment sizes were not small. Based on the sediment size prediction in Figure 41, the deposited sediments in the left split channel had d_{50} around 15 to 17 mm. It is possible that the neglect of lower flows (<4,000 cfs) contributed to the predicted deposition in the left split channel.

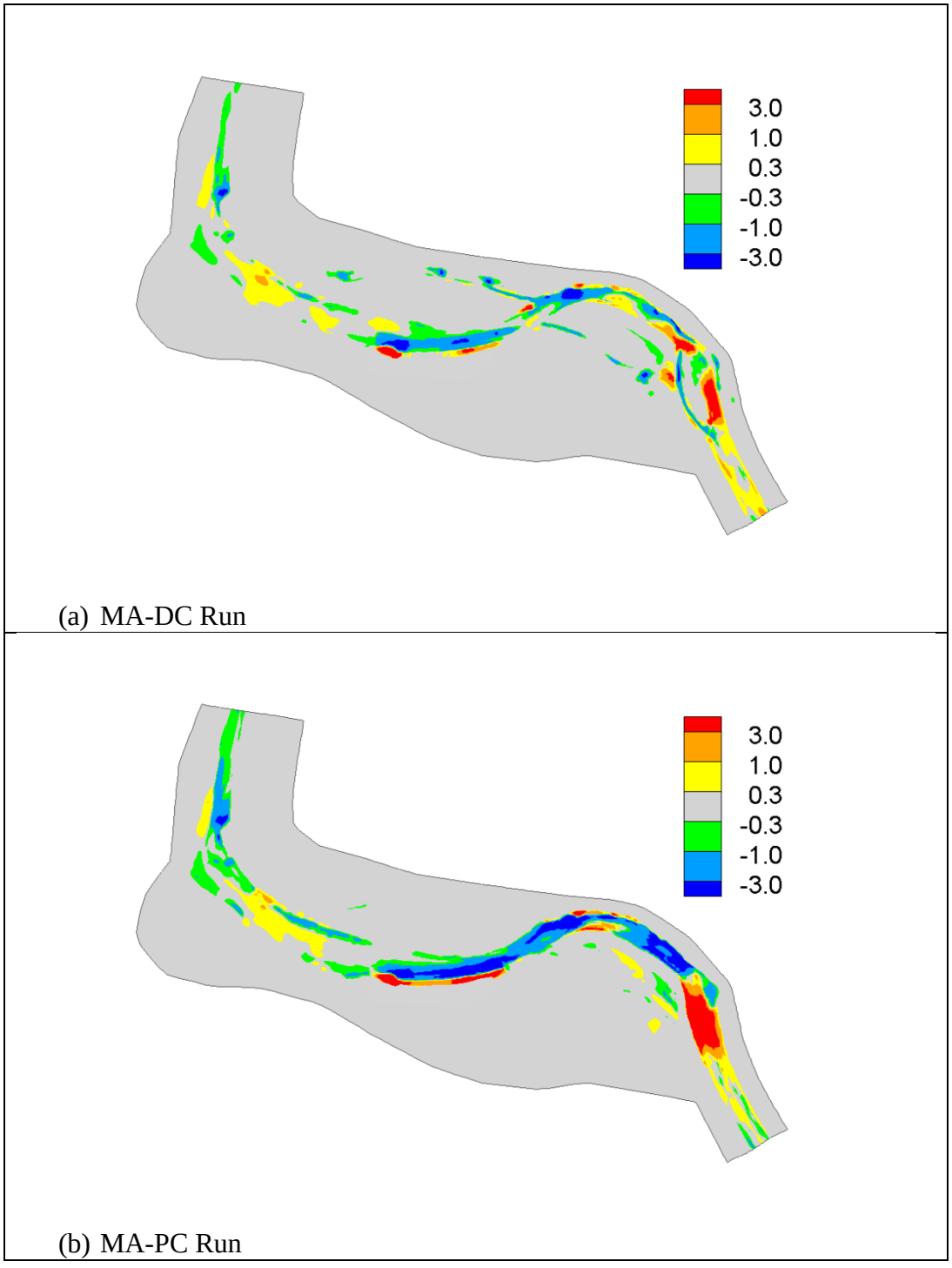

Figure 37. Predicted net erosion (positive) and deposition (negative) depth in feet with the 2012 design construction (DC) and 2011 post-erosion condition scenarios.

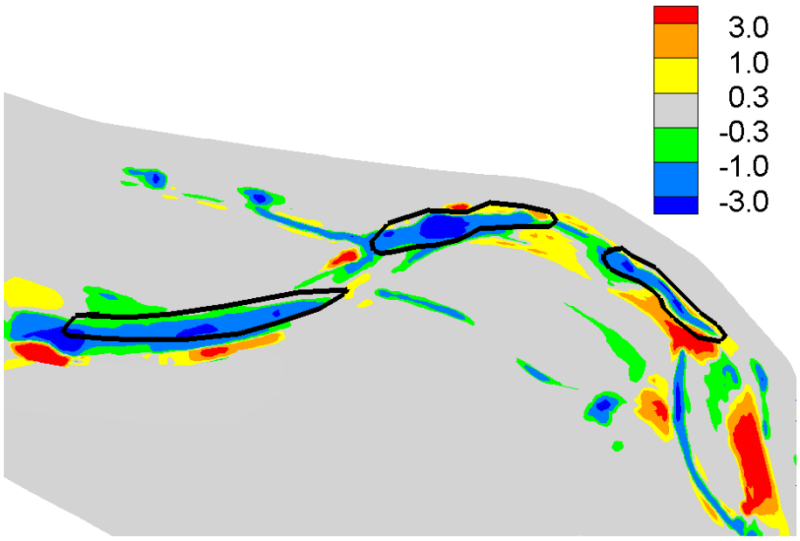

Figure 38. A zoom-in view of the predicted net erosion (positive) and deposition (negative) depth in feet with the MA-DC scenario (2012 design construction scenario.

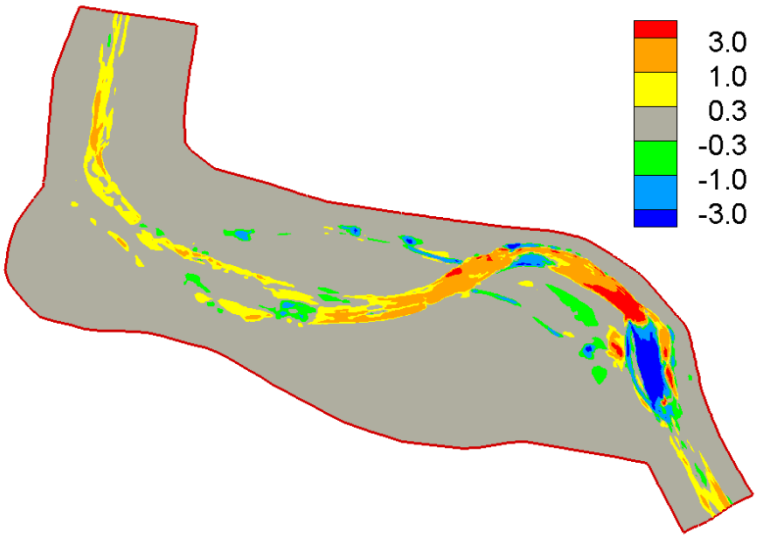

Figure 39. Differences of the predicted erosion and deposition depth in feet between MA-DC and MA-PC scenarios; positive if the design construction scenario predicted a lower bed elevation than the post-erosion condition scenario.

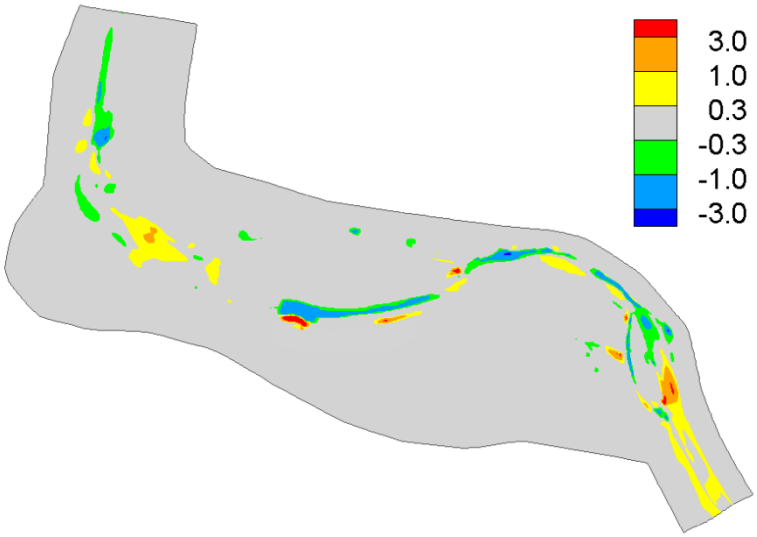

Figure 40. Predicted net erosion (positive) and deposition (negative) depth in feet with the MA-DC (design construction) after 2009 and 2010 runoffs.

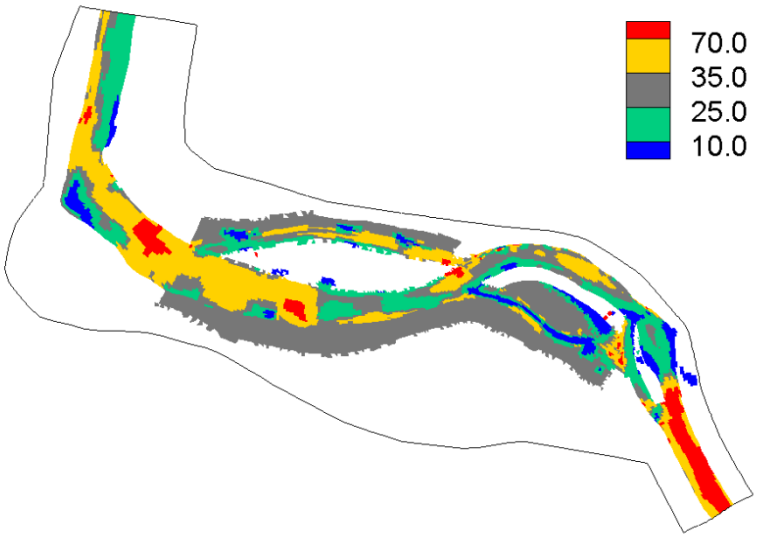

Figure 41. Predicted medium sediment diameter on the stream bed in August 2011.

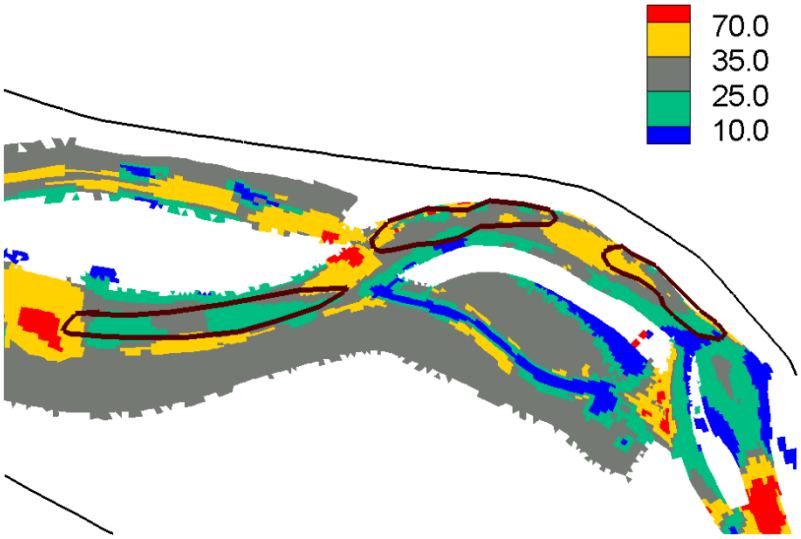

Figure 42. A zoom-in view of the predicted medium sediment diameter on the stream bed in August 2011.

7 References

Cardno ENTRIX. (2012). *Bank-Stability Analysis of the Upper Junction City Reach Trinity River, CA*, Project Report by Cardno Entrix, Project 30088130, December, 2012.

Gaeuman, D., Andrews, E.D., Krause, A., and Smith, W. (2009). "Predicting fractional bed load transport rates: Application of the Wilcock-Crowe equations to a regulated gravel bed river," Water Resour. Res., 45, W06409, doi:10.1029/2008WR007320.

Greimann, B.P., Lai, Y.G., and Huang, J., (2008). "Two-Dimensional Total Sediment Load Model Equations," J. Hydraulic Engineering, vol.134(8), 1142-1146.

Lai, Y.G., Weber, L.J., and Patel, V.C. (2003). "Non-hydrostatic three-dimensional method for hydraulic flow simulation - Part I: formulation and verification," J. Hydraul. Eng., ASCE, 129(3), 196-205.

Lai, Y.G. and Randle, T.J. (2007). *Bed Evolution and Bank Erosion Analysis of the Palo Verde Dam on the Lower Colorado River*. Technical Service Center, Bureau of Reclamation, Denver, CO.

Lai, Y.G. (2008). *SRH-2D Theory and User's Manual version 2.0,* Technical Service Center, Bureau of Reclamation, Denver, CO.

Lai, Y.G. and Greimann, B.P. (2008). "Modeling of erosion and deposition at meandering channels," World Environmental & Water Resources Congress, ASCE, May 12-16, 2008, Honolulu, Hawaii.

Lai, Y.G. (2010). "Two-Dimensional Depth-Averaged Flow Modeling with an Unstructured Hybrid Mesh," *J. Hydraulic Engineering*, ASCE, 136(1), 12-23.

Lai, Y.G. and Greimann, B.P. (2010). "Predicting contraction scour with a two-dimensional depth-averaged model," *J. Hydraulic Research*, IAHR, 48(3), 383-387.

Lai, Y.G., Greimann, B.P., and Wu, K. (2011). "Soft bedrock erosion modeling with a two-dimensional depth-averaged model," *J. Hydraulic Engineering*, ASCE, vol.137(8), pp.804-814.

Lai, Y.G., Thomas, R.E., Ozeren, Y., Simon, A., Greimann, B.P. and Wu, K. (2012a). "Coupling a two-dimensional model with a deterministic bank stability model." World Environmental & Water Resources Congress, May 20-24, 2012, Albuquerque, New Mexico.

Lai, Y.G., Greimann, B.P. and Wu, K. (2012b). "Modelling Bank Erosion in Fluvial Channels." River Flow 2012, International Conference on Fluvial Hydraulics, Sept. 5-7, San Jose, Costa Rica.

Lai, Y.G. (2013). *Bedload Adaptation Length for Modeling Bed Evolution in Gravel-Bed Rivers*. Report No. SRH-2013-15, Technical Service Center, Bureau of Reclamation, Denver, CO.

Logan, B., Nelson, J., McDonald, R., and Wright, S. (2010). "Mechanics and Modeling of Flow, Sediment Transport and Morphologic Change in Riverine Lateral Separation Zones," 2nd Joint Federal Interagency Conference, Las Vegas, NV, June 27 - July 1, 2010.

Parker, G., Seminara, G. and Solari, L. (2003). "Bed load at low Shields stress on arbitrarily sloping bed: Alternative entrainment formulation," *Water Resources Research*, 39(7),1183, doi:10.1029/2001WR001253.

Seminara, G., Solari, L., and Parker, G. (2002). "Bed load at low Shields stress on arbitrarily sloping beds: Failure of the Bagnold hypothesis," *Water Resources Research*, 38(11), 1249, doi:10.1029/2001WR000681.

Simon, A., Curini, A., Darby, S.E., Langendoen, E.J. (2000). Bank and near-bank processes in an incised channel, Geomorphology, 35(3-4): 193–217.

Simon, A., Pollen-Bankhead, N. and Thomas, R.E. (2011). Development and Application of a Deterministic Bank Stability and Toe Erosion Model for Stream Restoration. In: Simon, A., S.J. Bennett, J. Castro and C.R. Thorne (eds.), Stream Restoration in Dynamic Systems: Scientific Approaches, Analyses, and Tools. American Geophysical Union: Washington.

Wilcox, P.R. and Crowe, J.C. (2003). "Surface-Based Transport Model for Mixed-Size Sediment," J. Hydraulic Engineering, 129: 120-128.